AIMS Mathematics, 9(3): 7169–7211.
DOI: 10.3934/math.2024350
Received: 15 November 2023
Revised: 20 January 2024
Accepted: 25 January 2024
Published: 20 February 2024

http://www.aimspress.com/journal/Math

Research article

A new losses (revenues) probability model with entropy analysis, applications and case studies for value-at-risk modeling and mean of order-P analysis

Ibrahim Elbatal[1], L. S. Diab[1], Anis Ben Ghorbal[1], Haitham M. Yousof[2,*], Mohammed Elgarhy[3,4] and Emadeldin I. A. Ali[5,6]

[1] Department of Mathematics and Statistics, Faculty of Science, Imam Mohammad Ibn Saud Islamic University (IMSIU), Riyadh 11432, Saudi Arabia

[2] Department of Statistics, Mathematics and Insurance, Benha University, Benha, Egypt

[3] Department of Basic Sciences, Higher Institute of Administrative Sciences, Belbeis, AlSharkia, Egypt

[4] Mathematics and Computer Science Department, Faculty of Science, Beni-Suef University, Beni-Suef 62521, Egypt

[5] Department of Economics, College of Economics and Administrative Sciences, Imam Mohammad Ibn Saud Islamic University (IMSIU), Riyadh 11432, Saudi Arabia

[6] Department of Mathematics, Statistics, and Insurance, Faculty of Business, Ain Shams University, Egypt

* **Correspondence:** Email: haitham.yousof@fcom.bu.edu.eg.

Abstract: This study introduces the Inverse Burr-X Burr-XII (IBXBXII) distribution as a novel approach for handling asymmetric-bimodal claims and revenues. It explores the distribution's statistical properties and evaluates its performance in three contexts. The analysis includes assessing entropy, highlighting the distribution's significance in various fields, and comparing it to rival distributions using practical examples. The IBXBXII model is then applied to analyze risk indicators in actuarial data, focusing on bimodal insurance claims and income. Simulation analysis shows its preference for right-skewed data, making it suitable for mathematical modeling and actuarial risk assessments. The study emphasizes the IBXBXII model's versatility and effectiveness, suggesting it as a flexible framework for actuarial data analysis, particularly in cases of large samples and right-skewed data.

Keywords: asymmetric-bimodal claims data; asymmetric-bimodal insurance revenue data; losses (Gains) model; Tsallis entropy; value-at-risk; mean of order-P methodology
Mathematics Subject Classification: 62F15, 62G20, 65C60

1. Introduction

Insurance companies use historical data for risk assessment. Asymmetric-bimodal data analysis helps insurers understand varied risk levels and identify rare but severe events (tail risk) for better preparation. Analyzing claims data distribution improves claims management, fraud detection, and resource allocation. Reinsurance decisions, crucial for risk management, are guided by asymmetric-bimodal analysis. The introduced IBXBXII model efficiently addresses bimodal and asymmetric actuarial data, extending the adaptable BXII distribution commonly used in insurance. In summary, asymmetric-bimodal insurance data analysis facilitated by the IBXBXII model is vital for accurate risk assessment, pricing, compliance, and competitiveness, enabling data-driven decisions for financial stability and long-term success.These parameters can be adjusted to fit data with different shapes and tail characteristics (see [1–4]).

The BXII distribution assists insurers in setting premiums by offering insights into the potential distribution of claim amounts. In summary, the BXII distribution is a versatile tool in the insurance industry, influencing underwriting, reserving, solvency analysis, and risk transfer decisions. Its capacity to model various claim severities and capture tail risk makes it a valuable asset for assessing and managing risks associated with insurance claims. The following cumulative distribution function (CDF) is related to the BXII model:

$$F_{\alpha_1,\alpha_2}(z)|_{(z\geq 0)} = 1 - (z^{\alpha_2}+1)^{-\alpha_1}, \tag{1.1}$$

where both $\alpha_2 > 0$ and $\alpha_1 > 0$ controls the shape of the model. From Eq (1.1), if $\alpha_2 = 1$ ($\alpha_1 = 1$) we obtain the standard one-parameter Lomax (Lx) (the standard one-parameter log-logistic (LL) model). Details and many mathematical properties, applications, and more useful BXII extensions see [1–9]. Recently, many authors considered the extension of the BXII model such as [7] (beta BXII (B BXII)), [8] (Kumaraswamy BXII (KMBXII)) and [9] (Marshall-Olkin extended BXII (MOEBXII)), [10] (Marshall-Olkin Weibull-Burr XII), [11] (Compound class of unit Burr XII), [12] (Unit-Power Burr X), [13] (inverse exponentiated Lomax power series), [14] (Chen Burr-Hatke exponential), for more details [16–20]. After inverting the CDF of the type-X Burr-G (BX-G) family of [15], we substitute the CDF of the BXII model in (1.1), then the CDF of the IBXBXII model can be expressed as

$$F_{\zeta,\alpha_1,\alpha_2}(z) = 1 - \left(1 - \exp\left\{-\left[(z^{\alpha_2}+1)^{\alpha_1} - 1\right]^{-2}\right\}\right)^{\zeta}. \tag{1.2}$$

Staying in (1.2) and if $\zeta = 1$, we get the inverted Rayleigh BXII (IRBXII) model. For $\alpha_2 = 1$, we get the inverted BX Lomax (IBXLx) model. If $\alpha_1 = 1$, we get the inverted BX log-logistic (BXLL) model. For $\zeta = \alpha_2 = 1$, we get the inverted Rayleigh Lomax (IRLx) model. If $\zeta = \alpha_1 = 1$, we get the inverted Rayleigh log-logistic (IRLL) model. The PDF of the IBXBXII is given by

$$f_{\zeta,\alpha_1,\alpha_2}(z) = 2\zeta\alpha_1\alpha_2 z^{\alpha_1-1}\left[1-(z^{\alpha_2}+1)^{-\alpha_1}\right]^{-3}\frac{A_{\zeta,\alpha_1,\alpha_2}(z)(z^{\alpha_2}+1)^{-2\alpha_1-1}}{\exp\left\{\left[(z^{\alpha_2}+1)^{\alpha_1}-1\right]^{-2}\right\}}, \tag{1.3}$$

where $A_{\zeta,\alpha_1,\alpha_2}(z) = \left(1-\exp\left\{-\left[(z^{\alpha_2}+1)^{\alpha_1}-1\right]^{-2}\right\}\right)^{\zeta-1}$. The hazard rate function (HRF) of the IBXBXII model can be derived directly using (1.2) and (1.3) via the following formula $\frac{f_{\zeta,\alpha_1,\alpha_2}(z)}{1-F_{\zeta,\alpha_1,\alpha_2}(z)}$.

The updated distribution was applied in three ways. Firstly, it effectively evaluated entropy through four models, demonstrated via numerical comparisons. Secondly, its superior quality in various fields was highlighted by comparing it to competing distributions, particularly in applied modeling. Real-world applications were demonstrated with four datasets. Thirdly, the distribution analyzed actuarial data, assessing risks, and determining maximum insurance claims and revenue losses, showcasing its suitability for modeling and actuarial risk assessment, especially in right-skewed data. The IBXBXII model outperformed the MOOP estimator for positively skewed data but was surpassed for negatively skewed data. Regression analysis indicated a pronounced right skew, suggesting the distribution's preference for right-skewed insurance data. Computer simulations confirmed its effectiveness in mathematical modeling and actuarial risk assessments, showcasing its wide applicability against common distributions.

- The paper highlights the new distribution's versatility with four applications in medicine, engineering, dependability, and economics, showcasing its adaptability across diverse industries. Comparisons with established models in applied modeling reveal instances where the new distribution outperforms existing ones, providing valuable insights for practitioners. This aids in the selection of the most suitable distribution for specific needs, contributing to informed decision-making in various contexts.
- The study will compare the BXBXII distribution with various well-known BXII extensions, including Marshall-Olkin BXII (MARBXII), Topp-Leone BXII (TOLBXII), 5-paramters beta BXII (FBBXII), Beta BXII, beta exponentiated BXII (BEXBXII), 5-paramters Kumaraswamy BXII (FKMBXII), Zografos-Balakrishnan BXII (ZOBBXII), and Kumaraswamy modified BXII (KMBXII), in modeling veterinary medicine data (specifically, the survival times of guinea pigs). The evaluation will be based on criteria such as Akaike information, Bayesian information, Hannan-Quinn information, and Consistent Akaike information.
- The study focuses on modeling engineering data, specifically breaking stress data, through a comparison of the BXBXII distribution with various well-known BXII extensions. These extensions include the MARBXII distribution, TOLBXII distribution, ZOBBXII distribution, Beta BXII distribution, FKMBXII distribution. The assessment will employ criteria such as Akaike information, Bayesian information, Hannan-Quinn information, and Consistent Akaike information.
- In modeling econometrics data (the revenue data data), the BXBXII distribution will be compared with many well-known BXII extensions such as the standard BXII, MARBXII, TOLBXII, ZOBBXII, FBBXII, Beta BXII, BEXBXII, FKMBXII, and KMBXII distributions under the the Akaike information criteria (INFC), Bayesian INFC, Hannan-Quinn INFC, Consistent Akaike INFC.
- In modeling medicine data (the leukemia data), the BXBXII distribution will be compared with many well-known BXII extensions such as the standard BXII, MARBXII, TOLBXII, ZOBBXII, FBBXII, Beta BXII, BEXBXII, FKMBXII and KMBXII distributions under the Akaike INFC, Bayesian INFC, Hannan-Quinn INFC, Consistent Akaike INFC.
- The inclusion of two case studies, one on Value-at-Risk (VaR) modeling and the other on Mean of Order-P analysis underscores the practical relevance of the research. These case studies allow for the evaluation of the new distribution's performance in real-life scenarios, which can be invaluable for decision-makers and analysts.

The remaining parts of the paper can be structured in the following manner: Section 2 presents some properties. Section 3 gives some measures of entropy with numerical analysis. The main risk indicators are given in Section 4, the MOOP methodology for risk analysis is illustrated in Section 4. Section 5 presents a simulation study for assessing the estimation method. Section 6 offers a comparative study under four applications. Two actuarial case studies are presented in Section 7. Section 8 assesses the MOOP value at risk. Some conclusions are offered in Section 9.

2. Properties

2.1. *Exploring flexibility and the quantile function*

Figure 1 gives some plots of PDF for the IBXBXII distribution. Due to Figure 1, it is seen that the new PDF of the IBXBXII distribution can an unimodal PDF with a right tail. Figure 1 gives some plots of HRF for the IBXBXII distribution. Due to Figure 1, it is seen that the new HRF of the IBXBXII distribution can be J-HRF and upside-down HRF. Figure 1 illustrates the importance of the BXBXII distribution in modeling the real-life data sets that have upside-down HRF.

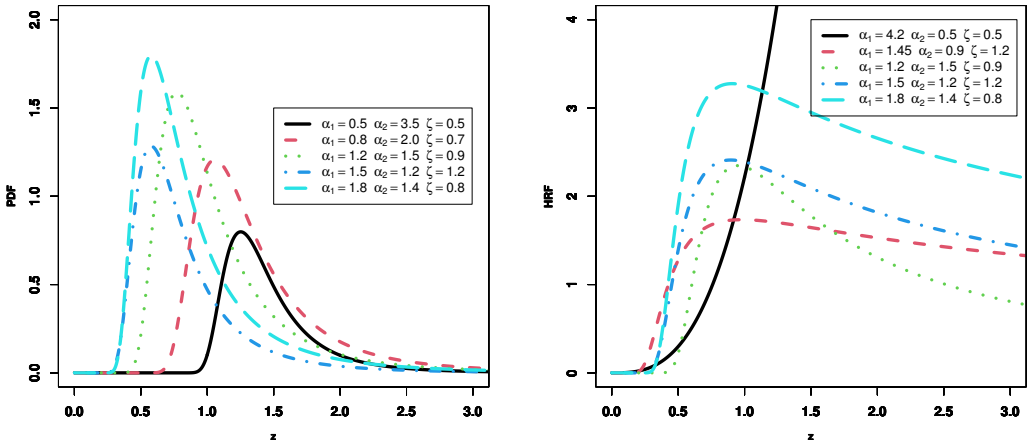

Figure 1. Plots of PDF and HRF for the IBXBXII distribution.

The quantile function (QF) of the new model is obtained by inverting (1.2) as $Q(u;\zeta,\alpha_1,\alpha_2) = F^{-1}(u;\zeta,\alpha_1,\alpha_2)$, $u \in (0,1)$. Then, the QF of the IBXBXII distribution is provided after some reductions by

$$Q(u;\zeta,\alpha_1,\alpha_2) = \left[\left(1+\left\{\log\left[1-(1-u)^{-\frac{1}{\zeta}}\right]\right\}^{\frac{1}{\alpha_2}}\right)^{\frac{1}{\alpha_1}} - 1\right]^{\frac{1}{\alpha_2}}. \tag{2.1}$$

Based (2.1), Bowley's skewness (γ_1) and Moor's kurtosis (γ_2) are given by

$$\gamma_1 = \frac{Q\left(\frac{7}{8};\zeta,\alpha_1,\alpha_2\right) - Q\left(\frac{5}{8};\zeta,\alpha_1,\alpha_2\right) + Q\left(\frac{3}{8};\zeta,\alpha_1,\alpha_2\right) - Q\left(\frac{1}{8};\zeta,\alpha_1,\alpha_2\right)}{Q\left(\frac{6}{8};\zeta,\alpha_1,\alpha_2\right) - Q\left(\frac{2}{8};\zeta,\alpha_1,\alpha_2\right)}, \tag{2.2}$$

and

$$\gamma_2 = \frac{Q\left(\frac{6}{8};\zeta,\alpha_1,\alpha_2\right) - 2Q\left(\frac{4}{8};\zeta,\alpha_1,\alpha_2\right) + Q\left(\frac{2}{8};\zeta,\alpha_1,\alpha_2\right)}{Q\left(\frac{6}{8};\zeta,\alpha_1,\alpha_2\right) - Q\left(\frac{2}{8};\zeta,\alpha_1,\alpha_2\right)}, \tag{2.3}$$

respectively. The plots of the γ_1 and γ_2 for the IBXBXII distribution is given in Figure 2 at $\zeta = 0.5$.

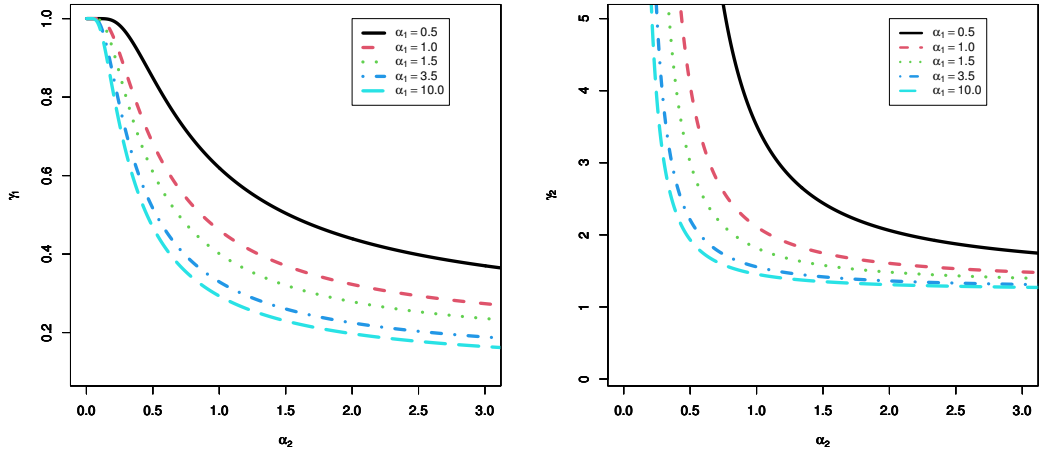

Figure 2. Plots of the γ_1 and γ_2 of the IBXBXII distribution at ζ =0.5.

2.2. *Moments*

If $\left|\frac{\nu_1}{\nu_2}\right| < 1$ and $\nu_3 > 0$ is a real non-integer, the following power series holds

$$\left(1 - \frac{\nu_1}{\nu_2}\right)^{\nu_3} = \sum_{\varsigma=0}^{\infty} (-1)^{\varsigma} \frac{\Gamma(1+\nu_3)}{\varsigma!\,\Gamma(1+\nu_3-\varsigma)} \left(\frac{\nu_1}{\nu_2}\right)^{\varsigma}. \tag{2.4}$$

Applying (2.4) to $A_{\zeta,\alpha_1,\alpha_2}(z)$ and inserting the expansion of $A_{\zeta,\alpha_1,\alpha_2}(z)$ into (1.3), we get

$$\begin{aligned} f_{\zeta,\alpha_1,\alpha_2}(z) &= 2\zeta\alpha_1\,\alpha_2 z^{\alpha_1-1}\left[1-(z^{\alpha_2}+1)^{-\alpha_1}\right]^{-3}(z^{\alpha_2}+1)^{-2\alpha_1-1} \\ &\quad \sum_{\varsigma=0}^{\infty} \frac{(-1)^{\varsigma}\,\Gamma(\zeta)}{\varsigma!\,\Gamma(\zeta-\varsigma)} \underbrace{\exp\left[-(\varsigma+1)\left[(z^{\alpha_2}+1)^{\alpha_1}-1\right]^{-2}\right]}_{B_{\varsigma,\alpha_1,\alpha_2}(z)}. \end{aligned} \tag{2.5}$$

Then, applying the power series to $B_{\varsigma,\alpha_1,\alpha_2}(z)$ and inserting the expansion of $B_{\varsigma,\alpha_1,\alpha_2}(z)$ into (2.5), the Eq (2.5) can be summarized as

$$\begin{aligned} f_{\zeta,\alpha_1,\alpha_2}(z) &= 2\zeta\alpha_1\,\alpha_2 z^{\alpha_1-1}\,(z^{\alpha_2}+1)^{-\alpha_1-1} \\ &\quad \times \sum_{\varsigma,\kappa=0}^{\infty} \frac{(-1)^{\varsigma+\kappa}\,(\varsigma+1)^{\kappa}\,\Gamma(\zeta)}{\varsigma!\,\kappa!\Gamma(\zeta-\varsigma)} \underbrace{\frac{[1-(z^{\alpha_2}+1)]^{-2\kappa-3}}{[(z^{\alpha_2}+1)]^{-2\kappa-1}}}_{B_{\kappa,\alpha_1,\alpha_2}(z)}. \end{aligned} \tag{2.6}$$

Applying (2.4) to $B_{\kappa,\alpha_1,\alpha_2}(z)$, Eq (2.6) can be written as

$$f_{\zeta,\alpha_1,\alpha_2}(z) = \sum_{\hbar=0}^{\infty} \mathbf{\Delta}_{\hbar} \mathbf{g}_{\alpha_1^*,\alpha_2}(z) \tag{2.7}$$

where

$$\mathbf{\Delta}_{\hbar} = \sum_{\varsigma,\kappa,j=0}^{\infty} 2\zeta \frac{(-1)^{\varsigma+\kappa+j+\hbar}\,(\varsigma+1)^{\kappa}\,\Gamma(\zeta)\,\Gamma(2\kappa+2)\,\Gamma(j-2(\kappa+1))}{\varsigma!\,\kappa!\,j!\hbar!\Gamma(\zeta-\varsigma)\,\Gamma(2\kappa+2-j)\,\Gamma(j-2(\kappa+1)-\hbar)\,(1+\hbar)},$$

and $\mathbf{g}_{\alpha_1^*,\alpha_2}(z) = \alpha_1^*\alpha_2 z^{\alpha_1-1}\,(z^{\alpha_2}+1)^{-\alpha_1^*-1}$ is the PDF of the BXII model with parameters $\alpha_1^* = \alpha_1(1+\hbar)$ and α_2. Similarly, the CDF of the IBXBXII can also be expressed as a mixture of BXII CDFs given by

$$F_{\zeta,\alpha_1,\alpha_2}(z) = \sum_{\hbar=0}^{\infty} \mathbf{\Delta}_{\hbar} \mathbf{G}_{\alpha_1^*,\alpha_2}(z)$$

where $\mathbf{G}_{\alpha_1^*,\alpha_2}(z)$ is the CDF of the BXII model with parameters α_1^* and α_2. Let W be a random variable having the BXII distribution with parameters α_1 and α_2. Then, the n^{th} ordinary and incomplete moments of W are, respectively, given by $\mu_n'|_{n<\alpha_1\alpha_2} = \alpha_1 B\left(\alpha_1 - \frac{n}{\alpha_2}, \frac{n}{\alpha_2}+1\right)$, and $\mathbf{\Upsilon}_n(z)|_{n<\alpha_1\alpha_2} = \alpha_1 B\left(z^{\alpha_2}; \alpha_1 - \frac{n}{\alpha_2}, \frac{n}{\alpha_2}+1\right)$, where $B(a_1,a_2) = \int_0^{\infty} t^{a_1-1}(1+t)^{-(a_1+a_2)}dt$, and $B(z;a_1,a_2) = \int_0^{z} t^{a_1-1}(1+t)^{-(a_1+a_2)}dt$ are the beta and the incomplete beta functions of the second type, respectively. So, several structural properties of the IBXBXII model can be obtained from (2.5) and those properties of the BXII distribution. The n^{th} ordinary moment of Z is given by

$$\mu_{n,Z}' = E(Z^n) = \sum_{\hbar=0}^{\infty} \mathbf{\Delta}_{\hbar} \int_0^{\infty} z^n\, \mathbf{g}_{\alpha_1^*,\alpha_2}(z)dz.$$

Then,

$$\mu_{n,Z}' = E(Z^n) = \sum_{\hbar=0}^{\infty} \mathbf{\Delta}_{\hbar}\alpha_1^* B\left(\alpha_1^* - \frac{n}{\alpha_2}, \frac{n}{\alpha_2}+1\right)|n<\alpha_1\alpha_2. \tag{2.8}$$

The n^{th} incomplete moment, say $\mathbf{\Upsilon}_s(t)$, of the IBXBXII distribution is given by

$$\mathbf{\Upsilon}_s(t) = \sum_{\hbar=0}^{\infty} \mathbf{\Delta}_{\hbar}\alpha_1^* B\left(t^{\alpha_2}; \alpha_1^* - \frac{s}{\alpha_2}, \frac{s}{\alpha_2}+1\right)|s<\alpha_1\alpha_2. \tag{2.9}$$

Table 1 gives expected value $(E(Z))$, variance $(V(Z))$, skewness $(S(Z))$ and kurtosis $(K(Z))$ for the IBXBXII model. Table 2 gives $E(Z)$, $V(Z)$, $S(Z)$ and $K(Z)$ for the BXII model. From Tables 1 and 2 we note that the $S_{\text{IBXBXII}}(Z)$ of the IBXBXII model $\in$ (-26.0701, 51.49378) however $S_{\text{BXII}}(Z)$ of the BXII model $\in$ (0.86282, 4.64757). The $K_{\text{IBXBXII}}(Z)$ of the IBXBXII model $\in$ (-602.017 to 2957.860) however the $K_{\text{BXII}}(Z)$ of the BXII model $\in$ (3.07, 73.80). Figure 3 (top left panel) gives 3D plot for the skewness of the IBXBXII distribution at $\zeta = 2.5$. Figure 3 (top right panel) presents 3D plot for the kurtosis of the IBXBXII distribution at $\zeta = 2.5$. Figure 3 (bottom right panel) shows 3D plot for the coefficient of variation (CV) of the IBXBXII distribution at $\zeta = 2.5$. Figure 3 (bottom left panel) displays 3D plot for the index of dispersion (ID) of the IBXBXII distribution at $\zeta = 2.5$. Based on Figure 3 (top left panel), we note that at $\zeta = 2.5$ the skewness of the IBXBXII distribution can have positive and negative values. Due Figure 3 (top right pane), it is seen that at $\zeta = 2.5$ the kurtosis of the

IBXBXII distribution is always positive and less that 3. According to Figure 3 (bottom right panel), we note that the CV of the IBXBXII distribution at $\zeta = 2.5$ can have U shape. According to Figure 3 (bottom left panel), it is concluded that the ID of the IBXBXII distribution at $\zeta = 2.5 \in (0, 1)$.

Table 1. $E(Z)$,$V(Z)$, $S(Z)$ and $K(Z)$ for the IBXBXII model.

ζ	α_1	α_2	$E(Z)$	$V(Z)$	$S(Z)$	$K(Z)$
1	3	2	0.81543166	0.022730081	1.607457	8.11645
20			0.62372778	0.000991441	0.032010	3.01156
50			0.60097949	0.000596520	-0.149218	3.01841
100			0.58720877	0.000432940	-0.252641	3.07572
500			0.56232022	0.000237130	-0.423748	3.25830
1000			0.55368533	0.000191146	-0.473076	3.15282
2000			0.54594558	0.000157149	-0.523666	3.41765
5000			0.53682011	0.000124283	-0.574841	3.51511
10000			0.53060272	0.000105681	-0.607892	3.58415
150	1	5	0.07414597	4.74804×10^{-5}	-0.133600	2957.86
	2		0.27199933	0.000162344	-0.274436	3.08417
	3		0.41969961	0.000172811	-0.322432	3.13870
	4		0.52139129	0.000150478	-0.346657	3.16935
	5		0.59389776	0.000125188	-0.361268	3.18888
3	1	1	0.8674569	0.110564801	2.297332	17.2822
		2	0.3617870	0.012992946	1.599782	8.576392
		5	0.1305731	0.001346009	1.308430	6.46725
		10	0.0631470	0.000291877	1.223986	16.9348
		25	0.0247642	4.29055×10^{-5}	-5.10736	113.501
		35	0.0176226	2.15464×10^{-5}	-26.0701	285.1312
		45	0.0136780	1.29135×10^{-5}	30.28077	-392.66
		50	0.0123013	1.04287×10^{-5}	51.49378	-602.02

Table 2. $E(Z)$, $V(Z)$, $S(Z)$ and $K(Z)$ for the BXII model.

a	b	$E(Z)$	$V(Z)$	$S(Z)$	$K(Z)$
1	5	0.250000	0.1041667	4.64751	73.8001
5		0.682424	0.0289951	0.040149	3.07002
15		0.873845	0.0058751	-0.553252	3.71623
35		0.942924	0.0013088	-0.755678	4.26811
50		0.959545	0.0006708	-0.804447	4.42885
75		0.972765	0.0003089	-0.843332	4.56514
100		0.979473	0.0001768	-0.862816	4.60851
		0.831252	0.0049489	-0.673595	3.83723
15	0.5	1.113879	0.0442417	2.131816	15.3416
	1	1.007348	0.0151023	0.598998	5.10838
	10	0.873846	0.0058750	-0.553252	3.71623
	25	0.780286	0.0041837	-0.742638	3.92925
	50	0.744512	0.0037574	-0.765126	3.96261
	100	0.710636	0.0034003	-0.776273	3.97973
	200	0.678424	0.0030882	-0.781829	3.98853
	500	0.638154	0.0027274	-0.785153	3.99380
	1000	0.609315	0.0024848	-0.786258	3.99556
	5000	0.547307	0.0020034	-0.787144	3.99698
	10000	0.522589	0.0018267	-0.787255	3.99832

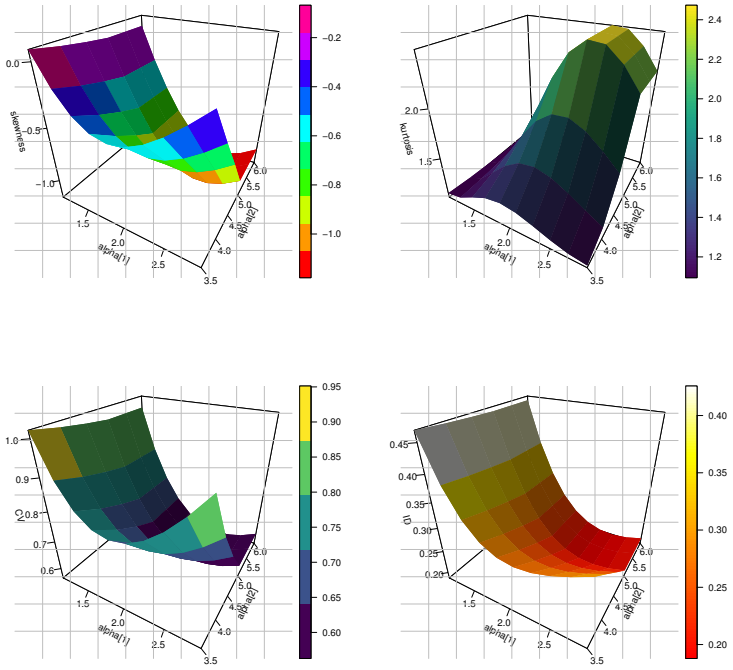

Figure 3. 3D plots for the IBXBXII distribution at $\zeta = 2.5$.

3. Measures of entropy

One of the most important measures of uncertainty is entropy. Many different types of entropy may be utilized to assess risk and reliability.

3.1. Rényi entropy

The Rényi entropy (RE) (see [28]) measure is determined using the following the following formula:

$$R_\omega = \frac{1}{1-\omega}\log\left[J_\omega(\zeta,\alpha_1,\alpha_2)\right],\ \omega>0,\omega\neq 1, \tag{3.1}$$

where $J_\omega(\zeta,\alpha_1,\alpha_2)=\int_0^\infty\left[f_{\zeta,\alpha_1,\alpha_2}(z)\right]^\omega dz$. Now we have to compute $J_\omega(\zeta,\alpha_1,\alpha_2)$. Then,

$$\begin{aligned}J_\omega(\alpha_1,\alpha_2,\zeta) &= (2\zeta\alpha_1\alpha_2)^\omega\int_0^\infty z^{w\alpha_1-\omega}(1+z^{\alpha_2})^{-2\omega\alpha_1-\omega}\left[1-(1+z^{\alpha_2})^{-\alpha_1}\right]^{-3\omega}\\ &\quad\times\exp\left\{-\omega\left[1-(1+z^{\alpha_2})^{-\alpha_1}\right]^{-2}\right\}\left(1-\exp\left\{-\omega\left[1-(1+z^{\alpha_2})^{-\alpha_1}\right]^{-2}\right\}\right)^{\omega\zeta-\omega}dz.\end{aligned}$$

By employing the binomial expansion to the last term in the above equation, we get

$$\begin{aligned}J_\omega(\alpha_1,\alpha_2,\zeta) &= (2\zeta\alpha_1\alpha_2)^\omega\sum_{i=0}^\infty(-1)^i\binom{\omega\zeta-\omega}{i}\int_0^\infty z^{w\alpha_1-\omega}(1+z^{\alpha_2})^{-2\omega\alpha_1-\omega}\\ &\quad\times\left[1-(1+z^{\alpha_2})^{-\alpha_1}\right]^{-3\omega}\exp\left\{-(i+1)\,\omega\left[1-(1+z^{\alpha_2})^{-\alpha_1}\right]^{-2}\right\}dz.\end{aligned}$$

By applying the exponential expansion to the last term in the last equation, we have

$$\begin{aligned}J_\omega(\zeta,\alpha_1,\alpha_2) &= (2\zeta\alpha_1\alpha_2)^\omega\sum_{\varsigma,j=0}^\infty(-1)^{\varsigma+j}\frac{\left[(\varsigma+1)\,\omega\right]^j}{j!}\binom{\omega\zeta-\omega}{\varsigma}\\ &\quad\times\int_0^\infty z^{w\alpha_1-\omega}(1+z^{\alpha_2})^{-2\omega\alpha_1-\omega}\left[1-(1+z^{\alpha_2})^{-\alpha_1}\right]^{-3\omega-2j}dz.\end{aligned}$$

Again utilizing the binomial theory, then

$$J_\omega(\zeta,\alpha_1,\alpha_2)=\sum_{\varsigma,j,k=0}^\infty\Im_{\varsigma,j,k}\int_0^\infty z^{w\alpha_1-\omega}(1+z^{\alpha_2})^{-(2\omega+k)\alpha_1-\omega}dz, \tag{3.2}$$

where

$$\Im_{\varsigma,j,k}=(-1)^{\varsigma+j}\frac{\left[(\varsigma+1)\,\omega\right]^j}{j!\,(2\zeta\alpha_1\alpha_2)^{-\omega}}\binom{\omega\zeta-\omega}{\varsigma}\binom{3\omega+2j+k-1}{k}.$$

Let $v=z^{\alpha_2}$, then

$$J_\omega(\zeta,\alpha_1,\alpha_2)=\sum_{\varsigma,j,k=0}^\infty\frac{\Im_{\varsigma,j,k}}{\alpha_2}\int_0^\infty v^{\frac{w\alpha_1}{\alpha_2}-\frac{\omega}{\alpha_2}+\frac{1}{\alpha_2}-1}(1+v)^{-(2\omega+k)\alpha_1-\omega}dv,$$

then

$$J_{\omega}(\zeta,\alpha_1,\alpha_2)=\sum_{\varsigma,j,k=0}^{\infty}\frac{\Im_{\varsigma,j,k}}{\alpha_2}B\left(\begin{array}{c}\varkappa(\alpha_1,\alpha_2;w,-\omega),\\ \left[\begin{array}{c}\varkappa(\alpha_1;\omega,k)\\ -\varkappa(\alpha_1,\alpha_2;w,\omega)\end{array}\right]\end{array}\right), \tag{3.3}$$

where $\varkappa(\alpha_1;\omega,k)=(2\omega+k)\alpha_1+\omega$ and $\varkappa(\alpha_1,\alpha_2;w,\omega)=\frac{w\alpha_1}{\alpha_2}+\frac{\omega}{\alpha_2}-\frac{1}{\alpha_2}>0$. Inserting (3.3) in (3.2), then the RE of the IBXBXII distribution is

$$R_{\omega}=\frac{1}{1-\omega}\log\left[\sum_{\varsigma,j,k=0}^{\infty}\frac{\Im_{\varsigma,j,k}}{\alpha_2}B\left(\begin{array}{c}\varkappa(\alpha_1,\alpha_2;w,-\omega),\\ \left[\begin{array}{c}\varkappa(\alpha_1;\omega,k)\\ -\varkappa(\alpha_1,\alpha_2;w,\omega)\end{array}\right]\end{array}\right)\right],\ \omega>0,\omega\neq1, \tag{3.4}$$

where $\varkappa(\alpha_1,\alpha_2;w,-\omega)=\frac{w\alpha_1}{\alpha_2}-\frac{\omega}{\alpha_2}+\frac{1}{\alpha_2}$. This approach can lead to more balanced and robust portfolios see [35, 36] for mare details.

3.2. Arimoto entropy

Due to [31], the Arimoto entropy (AE) measure is determined using the following the following formula:

$$A_{\omega}=\frac{\omega}{1-\omega}\left[(J_{\omega}(\zeta,\alpha_1,\alpha_2))^{\frac{1}{\omega}}-1\right],\ \omega>0,\omega\neq1. \tag{3.5}$$

Inserting (3.3) into (3.5), then the AE of the IBXBXII distribution is

$$A_{\omega}=\frac{\omega}{1-\omega}\left[\left(\sum_{\varsigma,j,k=0}^{\infty}\frac{\Im_{\varsigma,j,k}}{\alpha_2}B\left(\begin{array}{c}\varkappa(\alpha_1,\alpha_2;w,-\omega),\\ \left[\begin{array}{c}\varkappa(\alpha_1;\omega,k)\\ -\varkappa(\alpha_1,\alpha_2;w,\omega)\end{array}\right]\end{array}\right)\right)^{\frac{1}{\omega}}-1\right],\ \omega>0,\omega\neq1. \tag{3.6}$$

For more details see [32].

3.3. Tsallis entropy

The Tsallis entropy (TE) (see [31]) measure is determined using the following the following formula:

$$T_{\omega}=\frac{1}{\omega-1}\left[1-J_{\omega}(\zeta,\alpha_1,\alpha_2)\right],\ \omega>0,\omega\neq1. \tag{3.7}$$

Inserting (3.3) into (3.7), then the TE of the IBXBXII distribution is

$$T_{\omega}=\frac{1}{\omega-1}\left[1-\sum_{\varsigma,j,k=0}^{\infty}\frac{\Im_{\varsigma,j,k}}{\alpha_2}B\left(\begin{array}{c}\varkappa(\alpha_1,\alpha_2;w,-\omega),\\ \left[\begin{array}{c}\varkappa(\alpha_1;\omega,k)\\ -\varkappa(\alpha_1,\alpha_2;w,\omega)\end{array}\right]\end{array}\right)\right],\ \omega>0,\omega\neq1. \tag{3.8}$$

For more details see [35].

3.4. Havrda-Charvat entropy

Due to [25], the Havrda and Charvat entropy (HCE) measure is determined using the following the following formula:

$$HC_{\omega}=\frac{1}{2^{1-\omega}-1}\left[(J_{\omega}(\zeta,\alpha_1,\alpha_2))^{\frac{1}{\omega}}-1\right],\ \omega>0,\omega\neq1. \tag{3.9}$$

Inserting (3.3) into (3.9), then the HCE of the IBXBXII distribution is

$$HC_{\omega} = \frac{1}{2^{1-\omega}-1}\left[\left(\sum_{\varsigma,j,k=0}^{\infty}\frac{\Im_{\varsigma,j,k}}{\alpha_2}B\left(\begin{array}{c}\varkappa\left(\alpha_1,\alpha_2;w,-\omega\right),\\ \left[\begin{array}{c}\varkappa\left(\alpha_1;\omega,k\right)\\ -\varkappa\left(\alpha_1,\alpha_2;w,\omega\right)\end{array}\right]\end{array}\right)\right)^{\frac{1}{\omega}}-1\right],\ \omega>0,\omega\neq 1. \tag{3.10}$$

Havrda-Charvat entropy is a valuable tool for optimizing portfolio diversification by considering not only individual assets' risk and return but also their pairwise relationships, see [33] for more details. Tables 3 and 4 mention some numerical results of R_{ω}, A_{ω}, T_{ω}, and HC_{ω} for the IBXBXII distribution at ζ=2.0. Table 3 gives some numerical results of R_{ω}, HC_{ω}, T_{ω}, and A_{ω} for the IBXBXII distribution at ω = 0.3 and 0.6. Table 4 gives some numerical results of R_{ω}, HC_{ω}, T_{ω}, and A_{ω} for the IBXBXII distribution at ω = 1.2 and 2.0. We can note that from Tables 3 and 4 when α_2 is fixed and the values of α_1 are increases then the values of R_{ω}, A_{ω}, T_{ω} and HC_{ω} are decreases. Also, when α_1 is fixed and the values of α_2 are increases then the values of R_{ω}, A_{ω}, T_{ω}, and HC_{ω} are decreases. Also when α_1 and α_2 are fixed and ω is increase then the values of R_{ω}, A_{ω}, T_{ω}, and HC_{ω} are decreases.

Table 3. Some numerical results of R_{ω}, HC_{ω}, T_{ω}, and A_{ω} for the IBXBXII distribution at ω = 0.3 and 0.6.

α_2	α_1	ω = 0.3				ω = 0.6			
		R_{ω}	HC_{ω}	T_{ω}	A_{ω}	R_{ω}	HC_{ω}	T_{ω}	A_{ω}
1.5	0.5	0.831	137.364	4.022	36.765	-0.122	-0.534	-0.265	-0.256
	1.0	0.220	3.612	0.607	0.967	-0.337	-1.264	-0.667	-0.606
	1.2	0.115	1.369	0.291	0.366	-0.379	-1.382	-0.737	-0.662
	1.5	0.003	0.028	0.007	0.007	-0.425	-1.500	-0.810	-0.719
2	0.5	0.383	10.925	1.219	2.924	-0.465	-1.597	-0.871	-0.765
	1.0	0.029	0.266	0.067	0.071	-0.468	-1.604	-0.875	-0.769
	1.2	-0.038	-0.296	-0.085	-0.079	-0.464	-1.594	-0.869	-0.764
	1.5	-0.110	-0.713	-0.231	-0.191	-0.456	-1.575	-0.857	-0.755
2.5	0.5	0.146	1.907	0.379	0.510	-0.683	-2.034	-1.168	-0.975
	1.0	-0.097	-0.651	-0.207	-0.174	-0.564	-1.813	-1.013	-0.869
	1.2	-0.143	-0.861	-0.295	-0.230	-0.532	-1.747	-0.969	-0.837
	1.5	-0.193	-1.033	-0.382	-0.277	-0.493	-1.661	-0.912	-0.796
3	0.5	-0.014	-0.114	-0.031	-0.030	-0.840	-2.268	−1.347	-1.087
	1.0	-0.192	-1.030	-0.380	-0.276	-0.640	-1.959	-1.114	-0.939
	1.2	-0.225	-1.124	-0.435	-0.301	-0.591	-1.866	-1.049	-0.894
	1.5	-0.260	-1.206	-0.490	-0.323	-0.530	-1.743	-0.966	-0.835
3.5	0.5	-0.133	-0.819	-0.276	-0.219	-0.961	-2.414	−1.468	-1.157
	1.0	-0.268	-1.222	-0.501	-0.327	-0.705	-2.069	-1.194	-0.991
	1.2	-0.293	-1.269	-0.537	-0.340	-0.642	-1.962	-1.116	-0.940
	1.5	-0.318	-1.311	-0.573	-0.351	-0.567	-1.819	-1.017	-0.872

Table 4. Some numerical results of R_ω, HC_ω, T_ω, and A_ω for the IBXBXII distribution at ω = 1.2 and 2.

α_2	α_1	$\omega = 1.2$				$\omega = 2$			
		R_ω	HC_ω	T_ω	A_ω	R_ω	HC_ω	T_ω	A_ω
1.5	0.5	3.032	5.312	3.763	4.126	1.175	1.483	0.933	1.483
	1.0	1.690	3.687	2.704	2.864	0.468	0.833	0.659	0.833
	1.2	1.391	3.195	2.365	2.481	0.311	0.602	0.511	0.602
	1.5	1.044	2.551	1.909	1.981	0.130	0.278	0.259	0.278
2	0.5	3.221	5.481	3.866	4.257	1.105	1.440	0.922	1.440
	1.0	1.508	3.394	2.503	2.636	0.327	0.627	0.529	0.627
	1.2	1.123	2.704	2.018	2.100	0.153	0.323	0.297	0.323
	1.5	0.676	1.765	1.338	1.371	-0.047	-0.112	-0.115	-0.112
2.5	0.5	3.307	5.553	3.909	4.313	1.041	1.397	0.909	1.397
	1.0	1.373	3.164	2.343	2.457	0.220	0.447	0.397	0.447
	1.2	0.937	2.333	1.752	1.812	0.036	0.081	0.080	0.081
	1.5	0.430	1.176	0.899	0.914	-0.176	-0.449	-0.499	-0.449
3	0.5	3.347	5.587	3.930	4.339	0.983	1.355	0.896	1.355
	1.0	1.267	2.974	2.210	2.310	0.134	0.285	0.265	0.285
	1.2	0.797	2.035	1.536	1.581	-0.057	-0.135	-0.139	-0.135
	1.5	0.251	0.709	0.546	0.551	-0.276	-0.749	-0.890	-0.749
3.5	0.5	3.364	5.601	3.938	4.350	0.932	1.316	0.883	1.316
	1.0	1.180	2.814	2.096	2.185	0.062	0.137	0.133	0.137
	1.2	0.686	1.788	1.355	1.389	-0.133	-0.331	-0.359	-0.331
	1.5	0.112	0.324	0.251	0.252	-0.359	-1.022	-1.284	-1.022

4. Main risk indicators

In this work, we consider the main four indicators of risks called the value-at-risk ($\mathbb{V}_1$), tail value-at-risk ($\mathbb{V}_2$), tail variance ($\mathbb{V}_3$) and tail mean variance ($\mathbb{V}_4$). These indicators are used for analyzing the actuarial data sets below. Let Z denotes a random variable of losses (or gains). The value-at-risk of Z at the $100q\%$ level, say $\mathbb{V}_1$ or $\pi(q)$, is the $100q\%$ quantile of the distribution of Z under the IBXBXII distribution can be expressed as:

$$\mathbb{V}_1 = \Pr\left(Z > Q\left(u;\zeta,\alpha_1,\alpha_2\right)\right) | \left(q = 99\%\right) = 1\%.$$

According to [34], the indicator $\mathbb{V}_1$ satisfies all coherence requirements if the distribution of losses (or distribution of gains) is restricted to the normal distribution. In most cases, the data sets that deal with insurance have a bias either toward the left or the right, and on occasion, it is bimodal. Because of this, it is inappropriate to apply the normal distribution to the process of describing insurance claims. For this purpose, the indicator $\mathbb{V}_2$ may be a useful indicator in such cases, where

$$\mathbb{V}_2 = \frac{1}{1-q}\varsigma\left(Z;\pi\left(q\right),\infty\right),$$

where $\varsigma\left(Z;\pi\left(q\right),\infty\right)=\int\limits_{\pi(q)}^{\infty}z\,f_{\zeta,\alpha_1,\alpha_2}\left(z\right)dz$. Then,

$$\mathbb{V}_2=\frac{\alpha_1}{1-q}\sum_{\hbar=0}^{\infty}\mathbf{\Delta}_{\hbar}\left(1+\hbar\right)\left[\begin{array}{c}B\left(\alpha_1^*-\frac{1}{\alpha_2},\frac{1}{\alpha_2}+1\right)\\-B\left(\pi\left(q\right)^{\alpha_2};\alpha_1^*-\frac{1}{\alpha_2},\frac{1}{\alpha_2}+1\right)\end{array}\right]|1<\alpha_1\alpha_2,$$

where $B\left(\pi\left(q\right)^{\alpha_2};\alpha_1^*-\frac{1}{\alpha_2},\frac{1}{\alpha_2}+1\right)>0$. The indicator $\mathbb{V}_2$ refers to average of all $\mathbb{V}_1$ at the confidence level q, which means that the indicator $\mathbb{V}_2$ provides more actuarial information about the tail of the IBXBXII distribution, see [29]. Due to [29, 30] it can also be expressed as $\mathbb{V}_2=\mathbb{V}_1+e\left(\mathbb{V}_1\right)$, where $e\left(\mathbb{V}_1\right)$ is the function of mean excess loss evaluated at the $100q\%$th quantile. [24] presented an explicit expressions for the indicator $\mathbb{V}_2$ indicator under the multivariate normal distribution, the indicator $\mathbb{V}_2$ under the IBXBXII distribution can be obtained as

$$\mathbb{V}_3=\mathbb{V}\left[Z^2;\pi\left(q\right)\right]-\mathbb{V}_2^2,$$

where

$$\mathbb{V}\left[Z^2;\pi\left(q\right)\right]=\alpha_1\sum_{\hbar=0}^{\infty}\mathbf{\Delta}_{\hbar}\left(1+\hbar\right)\left[\begin{array}{c}B\left(\alpha_1^*-\frac{2}{\alpha_2},\frac{2}{\alpha_2}+1\right)\\-B\left(\pi\left(q\right)^{\alpha_2};\alpha_1^*-\frac{2}{\alpha_2},\frac{2}{\alpha_2}+1\right)\end{array}\right]|2<\alpha_1\alpha_2,$$

where $B\left(\pi\left(q\right)^{\alpha_2};\alpha_1^*-\frac{2}{\alpha_2},\frac{2}{\alpha_2}+1\right)>0$. Finally, due to [26], the $\mathbb{V}_4$ indicator can be estimated from

$$\mathbb{V}_4=\mathbb{V}_2+\pi\mathbb{V}_3|_{0<\pi<1}.$$

According to [23], the Mean of Order-P (MOOP) methodology serves as an alternative approach in value-at-risk (VaR) analysis, offering a distinct perspective by considering the order or rank of returns. VaR is a widely used risk management statistic to quantify potential investment or portfolio losses over a specific time horizon with a certain confidence level.

5. Assessing the estimation method

Let $\underline{\Theta}=(\zeta,\alpha_1,\alpha_2)^{\intercal}$ be the parameter vector of our model. For determining the maximum likelihood estimations (MAXLE) of $\underline{\Theta}$, we deriving the log-likelihood function ($\ell_{\zeta,\alpha_1,\alpha_2}$). The goal of this section is to investigate the MAXLE's behavior, which was addressed in the previous section. The Monte Carlo analysis is used to assess the efficacy of the recommended estimate methods. R, a statistical programming language, will be used to do the calculation. The Monte Carlo simulation is done using a variety of approved estimating approaches. Under the following assumptions, the IBXBXII distribution may be used to generate a thousand random data elements:

Step 1: Generated random data of the IBXBXII distribution from Eq (2.1) with α_1, α_2, and ζ given sample size n = 25, 50, 100, 200 and 300.

Step 2: Calculate the MLEs of α_1, α_2, and ζ utilizing the true value of these parameters.

Step 3: Repeating Step 1 to Step 1 number of times 5000 and saving all estimates.

Step 4: Calculating the statistical measures of performance for point and interval estimates: Mean square errors (C_1), lower limit (C_2), upper limit (C_3) of 90% and 95% confidence interval and average length (C_4).

All the results of the Monte Carlo simulation for each case for the given parameters: $(\zeta, \alpha_1, \alpha_2)$ are reported in Tables 5–8. From these tabulated values, one can indicate that: As n increases, the C_2 and C_4 decreases.

Table 5. Point and interval simulation results for the IBXBXII distribution at α_1=0.5, α_2=1.5 and ζ=0.5.

n		MAXLE	C_1	90%			95%		
				C_2	C_3	C_4	C_2	C_3	C_4
25	α_1	0.5192	0.1137	0.3513	0.6871	0.3358	0.3192	0.7193	0.4001
	α_2	2.0599	1.7948	-3.0266	7.1465	10.1731	-4.0006	8.1205	12.1211
	ζ	0.4743	0.2179	-0.6169	1.5655	2.1824	-0.8258	1.7745	2.6003
50	α_1	0.4991	0.0909	0.3707	0.6275	0.2568	0.3462	0.6521	0.3059
	α_2	2.4692	1.4596	-1.7495	6.6879	8.4375	-2.5574	7.4958	10.0532
	ζ	0.3758	0.2129	-0.4399	1.1915	1.6314	-0.5961	1.3477	1.9438
100	α_1	0.4618	0.0056	0.3841	0.5994	0.2153	0.3635	0.6200	0.2565
	α_2	1.7169	1.4084	-2.0831	5.5169	7.6000	-2.8108	6.2446	9.0554
	ζ	0.5191	0.0754	-0.3177	1.3560	1.6737	-0.4780	1.5162	1.9942
200	α_1	0.4877	0.0023	0.4035	0.5718	0.1683	0.3874	0.5879	0.2006
	α_2	1.6821	1.2229	-1.0977	4.4620	5.5596	-1.6300	4.9943	6.6242
	ζ	0.4948	0.0590	-0.0846	1.0741	1.1587	-0.1955	1.1851	1.3806
300	α_1	0.5039	0.0012	0.4400	0.5679	0.1279	0.4277	0.5801	0.1524
	α_2	1.5210	1.1090	-0.7268	4.5688	5.2956	-1.2338	5.0759	6.3097
	ζ	0.4420	0.0330	-0.0766	0.9605	1.0371	-0.1759	1.0598	1.2356

Table 6. Point and interval simulation results for the IBXBXII distribution at α_1=0.9, α_2=0.6 and ζ=0.4.

n		MAXLE	C_1	90%			95%		
				C_2	C_3	C_4	C_2	C_3	C_4
25	α_1	0.9048	0.1077	0.6901	1.1195	0.4294	0.6489	1.1606	0.5117
	α_2	0.5067	1.1646	-2.5296	3.5430	6.0725	-3.1110	4.1244	7.2354
	ζ	0.4638	0.1774	0.0255	0.9022	0.8767	-0.0585	0.9861	1.0446
50	α_1	0.9051	0.0702	0.7366	1.0736	0.3370	0.7043	1.1059	0.4015
	α_2	0.7728	1.0684	-1.2408	3.4664	4.7073	-1.6915	4.9171	6.6086
	ζ	0.3462	0.1479	0.0636	0.8288	0.7652	0.0095	0.8830	0.8734
100	α_1	0.9152	0.0559	0.7910	1.0395	0.2485	0.7672	1.0632	0.2961
	α_2	0.7666	0.5973	-1.9020	2.4352	4.3372	-2.4130	3.9462	6.3592
	ζ	0.3758	0.1153	0.0245	0.7271	0.7026	-0.0427	0.7944	0.8371
200	α_1	0.8843	0.0444	0.8447	1.0239	0.1792	0.8180	1.0507	0.2327
	α_2	0.3641	0.4164	-1.4883	2.2165	3.7048	-1.8430	2.5712	4.4142
	ζ	0.4642	0.1076	0.2013	0.7271	0.5258	0.1510	0.7775	0.6265
300	α_1	0.9025	0.0386	0.8125	0.9926	0.1801	0.7952	1.0099	0.2146
	α_2	0.6634	0.6231	-0.8207	2.1476	2.9683	-1.1049	2.4318	3.5367
	ζ	0.4097	0.0875	0.1937	0.6258	0.4322	0.1523	0.6672	0.5149

Table 7. Point and interval simulation results for the IBXBXII distribution at α_1=0.8, α_2=0.5 and ζ=0.5.

n		MAXLE	C_1	90%			95%		
				C_2	C_3	C_4	C_2	C_3	C_4
25	α_1	0.7908	0.0998	0.6261	0.9555	0.3295	0.5945	0.9871	0.3925
	α_2	0.9671	1.0789	-1.6168	3.5511	5.1679	-2.1116	4.0459	6.1575
	ζ	0.3983	0.2643	0.0141	0.7825	0.7684	-0.0595	0.8561	0.9156
50	α_1	0.8171	0.0621	0.6729	0.9613	0.2884	0.6453	0.9889	0.3437
	α_2	0.7095	1.1214	-1.5445	2.9635	4.5080	-1.9761	3.3951	5.3712
	ζ	0.5095	0.2376	0.1477	0.8713	0.7237	0.0784	0.9406	0.8622
100	α_1	0.8046	0.0321	0.6921	0.9171	0.2250	0.6705	0.9386	0.2681
	α_2	0.8810	0.9905	-1.2841	3.0461	4.3301	-1.6987	3.4606	5.1593
	ζ	0.4517	0.1712	0.1169	0.7864	0.6695	0.0528	0.8505	0.7978
200	α_1	0.7986	0.0689	0.6889	0.9082	0.2193	0.6679	0.9292	0.2613
	α_2	0.6635	1.2782	-1.3298	2.6569	3.9867	-1.7116	3.0386	4.7502
	ζ	0.5313	0.2214	0.2273	0.8353	0.6079	0.1691	0.8935	0.7243
300	α_1	0.8106	0.0556	0.7312	0.8901	0.1590	0.7159	0.9054	0.1894
	α_2	0.6300	0.8947	-0.7001	1.9601	2.6601	-0.9548	2.2148	3.1695
	ζ	0.5055	0.1442	0.2834	0.7275	0.4441	0.2409	0.7701	0.5292

Table 8. Point and interval simulation results for the IBXBXII distribution at α_1=α_2=ζ=0.5.

n		MAXLE	C_1	90%			95%		
				C_2	C_3	C_4	C_2	C_3	C_4
25	α_1	0.4927	0.0827	0.2777	0.9078	0.6301	0.1557	0.9298	0.7742
	α_2	0.3132	0.7077	-1.6453	2.2718	3.9171	-2.0204	2.6468	4.6672
	ζ	0.5506	0.1466	0.1563	0.9448	0.7886	0.0808	1.0204	0.9396
50	α_1	0.4832	0.0792	0.1100	0.6563	0.5463	0.1960	0.8703	0.6743
	α_2	0.3960	1.2828	-1.1539	1.9458	3.0997	-1.4506	2.2426	3.6932
	ζ	0.4989	0.1361	0.2249	0.7729	0.5480	0.1725	0.8254	0.6529
100	α_1	0.6019	0.0192	0.3433	0.8606	0.5173	0.2938	0.9101	0.6164
	α_2	0.6360	0.2203	-0.0396	1.3117	1.3514	-0.1690	1.4411	1.6101
	ζ	0.5470	0.0173	0.3951	0.6990	0.3039	0.3660	0.7281	0.3621
200	α_1	0.4839	0.0172	0.3544	0.6335	0.2791	0.3277	0.6602	0.3325
	α_2	0.4683	0.1218	0.1140	0.7625	0.6485	0.0519	0.8246	0.7727
	ζ	0.5418	0.0139	0.4391	0.6845	0.2454	0.4156	0.7080	0.2924
300	α_1	0.5197	0.0065	0.4109	0.6685	0.2576	0.3862	0.6931	0.3069
	α_2	0.4841	0.0130	0.1768	0.7515	0.5747	0.1217	0.8065	0.6848
	ζ	0.5113	0.0052	0.4590	0.6436	0.1846	0.4413	0.6613	0.2199

6. Reliability, economic, and medical data sets for comparing models

Now, in order to illustrate how flexible the IBXBXII model is, we will provide four applications to four distinct collections of real data. These applications will highlight how the model may be applied to a variety of situations. For the four real-life economic, reliability, and medical data sets, we compare the IBXBXII distribution, with the standard BXII, MARBXII, TOLBXII, ZOBBXII, FBBXII, Beta BXII, BEXBXII, FKMBXII and KMBXII distributions. We consider the following well-known statistic tests (information criterion (INFC)): The Akaike INFC ($\mathbb{C}_{\mathrm{AI}}$), Bayesian INFC ($\mathbb{C}_{\mathrm{BYS}}$), Hannan-Quinn INFC ($\mathbb{C}_{\mathrm{HQ}}$), Consistent Akaike INFC ($\mathbb{C}_{\mathrm{CA}}$). The data set I (reliability data) refers to the breaking stress data (see [27]. The data set II (reliability data) presents survival times of guinea pigs see [21]). The data set III is taxes revenue data (economic data). The data set IV is called leukemia data (medical data). Plots and box plots, Quantile-Quantile "(Q-Q) plots, the total time in test (TTT)" plots, and the "Kernel density" are some of the many helpful graphical tools that are utilized. The Kernel density for each of the four different data sets is presented in Figure 4. The TTT for each of the four data sets is represented in Figure 5, which may be found below. In Figure 6, the Q-Q is presented for each of the four data sets individually. Box plots for each of the four genuine data sets are shown in Figure 7, which may be found here. The "box plot" is used to look for and identify outliers, which are defined as extreme observations (see Figures 6 and 7). The Q-Q plot, which can be found in Figure 6, is used to evaluate the "normality" of the four different real data sets. Through the utilization of the TTT tool, the initial HRF form can be investigated (see Figure 5). Exploration of the first PDF shape can be accomplished with the help of the Kernel density tool (see Figure 4).

According to Figure 4, it can be seen that the Kernel density has the shape of a bimodal distribution with a heavy tail for data set II, data set III, and data set IV respectively. The HRF is seen to be

"monotonically increasing" for data set I, data set II, and data set III, and it is shown to be a bathtub HRF (U-HRF) for data set IV based on what is seen in Figure 5. It can be seen from Figure 6 that both data set II and data set III contain some values that are on the extreme end of the scale. On the other hand, neither data Set I nor data set IV have any numbers that are particularly extreme. Additionally, it can be demonstrated that the "normality" may be present for the data sets I and III. Figure 7 provides evidence that the findings presented in Figure 2 are accurate; yet, because of Figure 2 (the panel on the top right), it is clear that there is an extreme value. Figure 8's top right panel displays the estimated probability density function (EPDF) for data sets I. The EPDF for data set II can be found in the panel located in the top left corner of Figure 8. The EPDF for data set III can be found in the panel located in the bottom right corner of Figure 8. The EPDF for data set IV can be found in the panel located in the bottom right corner of Figure 8. As a result of examining Figure 8, we have reached the conclusion that the IBXBXII model offers an appropriate fitting to the histograms of all four data sets. The empirical and theoretical CDFs for data set I are presented in the panel located in the upper right-hand corner of Figure 9. The empirical and theoretical CDFs plot for data set II can be found in the panel located in the top left corner of Figure 9. The empirical and theoretical CDFs plot for data sets III may be seen in the panel located in the bottom right corner of Figure 9. The empirical and theoretical CDFs shown for data set IV can be seen in the panel located in the bottom right corner of Figure 9. The probability-probability (P-P) ratio for data set I is displayed in the panel located in the upper right corner of Figure 10. The P-P plot for data set II may be seen in the panel located in the top left corner of Figure 10. The P-P plot for data set III may be found in the panel located in the bottom right corner of Figure 10. The P-P plot for data set IV may be found in the panel located in the bottom right corner of Figure 10. The Kaplan-Meier survival analysis for data set I may be seen in the panel on the upper right of Figure 11. The Kaplan-Meier survival plot (KMSP) for data set II is displayed in the panel located in the top left corner of Figure 11. The KMSP for data set III can be seen in the panel located in the bottom right corner of Figure 11. The KMSP for data set IV can be seen in the panel located in the bottom right corner of Figure 11. As a result of examining Figure 8, we have reached the conclusion that the IBXBXII offers an appropriate fitting to all four data sets. The KMSP for data sets I is displayed in the panel located in the top right corner of Figure 9. The KMSP for data set II may be seen in the panel located in the top left corner of Figure 9. The KMSP for data set III can be seen in the panel located in the bottom right corner of Figure 9. The KMSP for data set IV can be seen in the panel located in the bottom right corner of Figure 9. As a result of looking at Figure 8, we have come to the conclusion that the IBXBXII offers an appropriate fitting to the empirical survival functions for all four data sets.

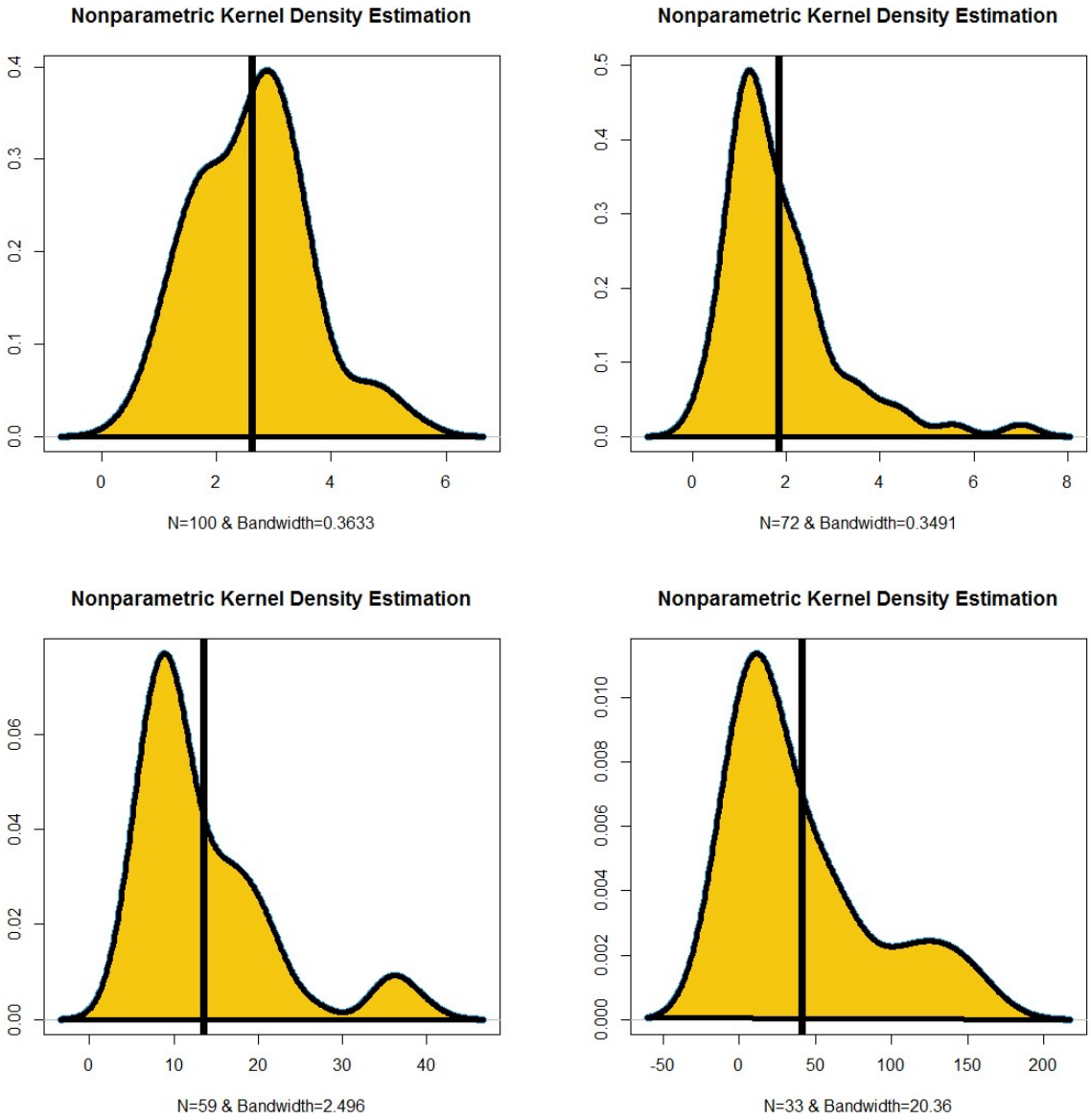

Figure 4. NKDE plots.

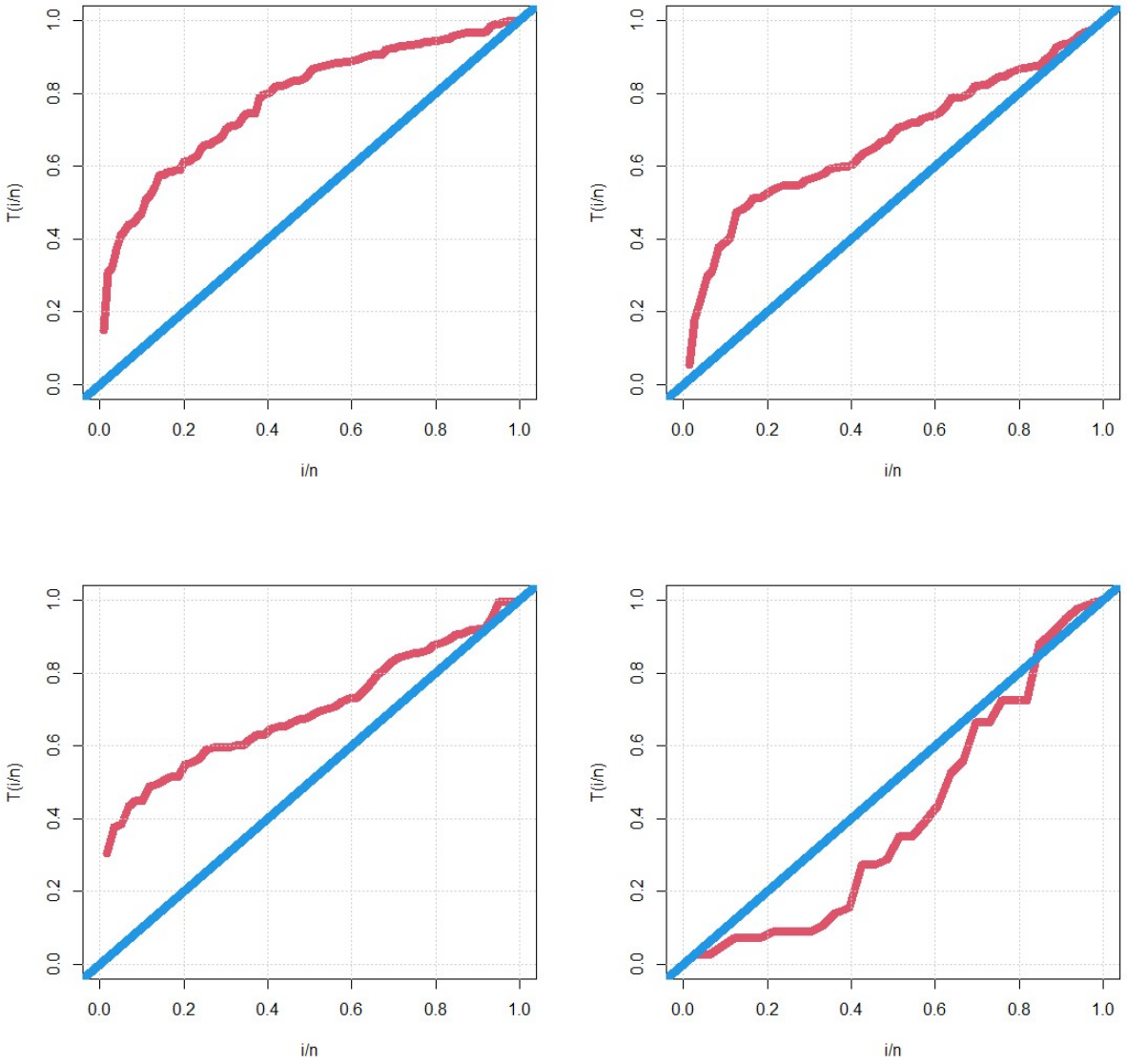

Figure 5. TTT plots.

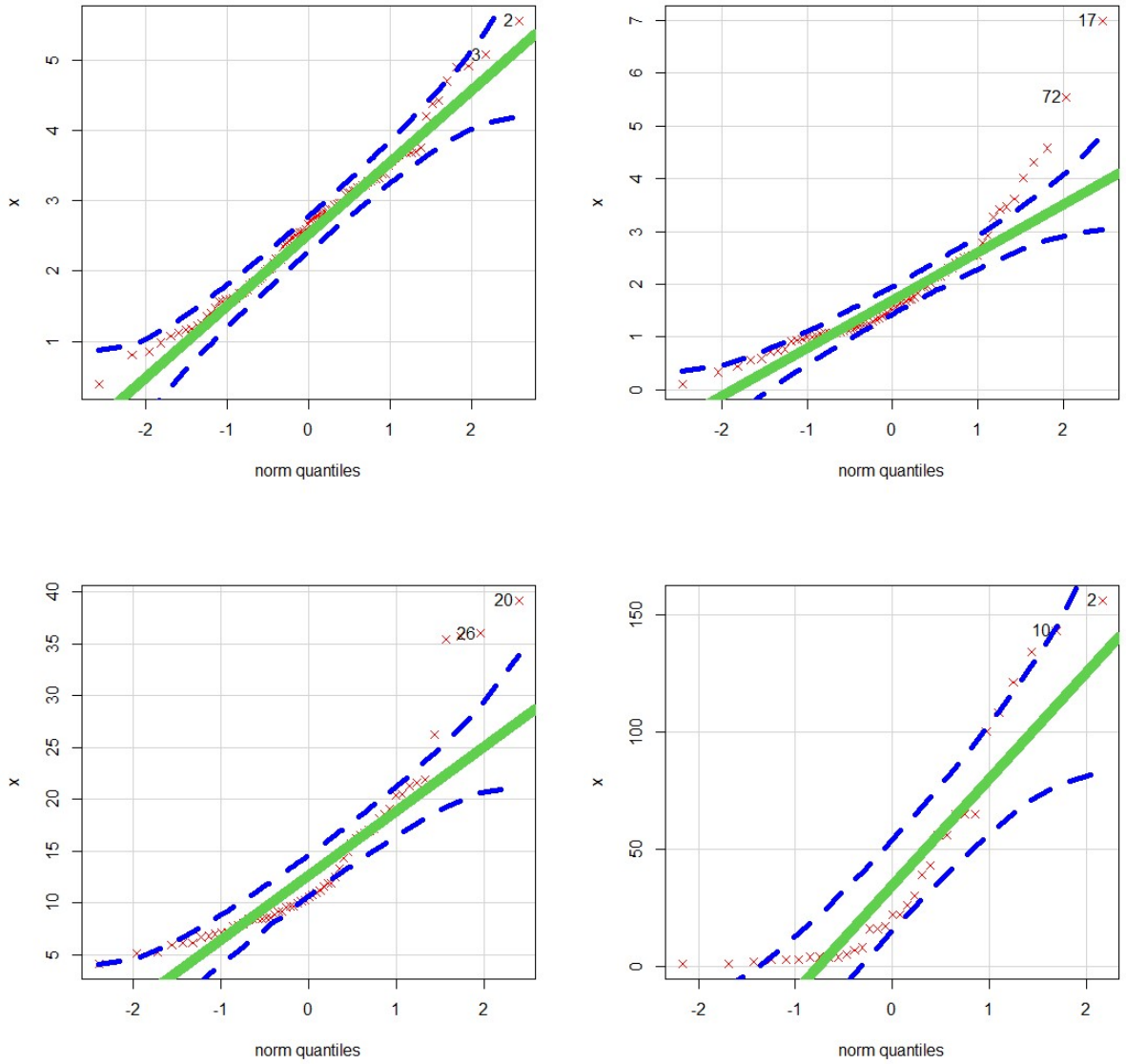

Figure 6. Q-Q plots.

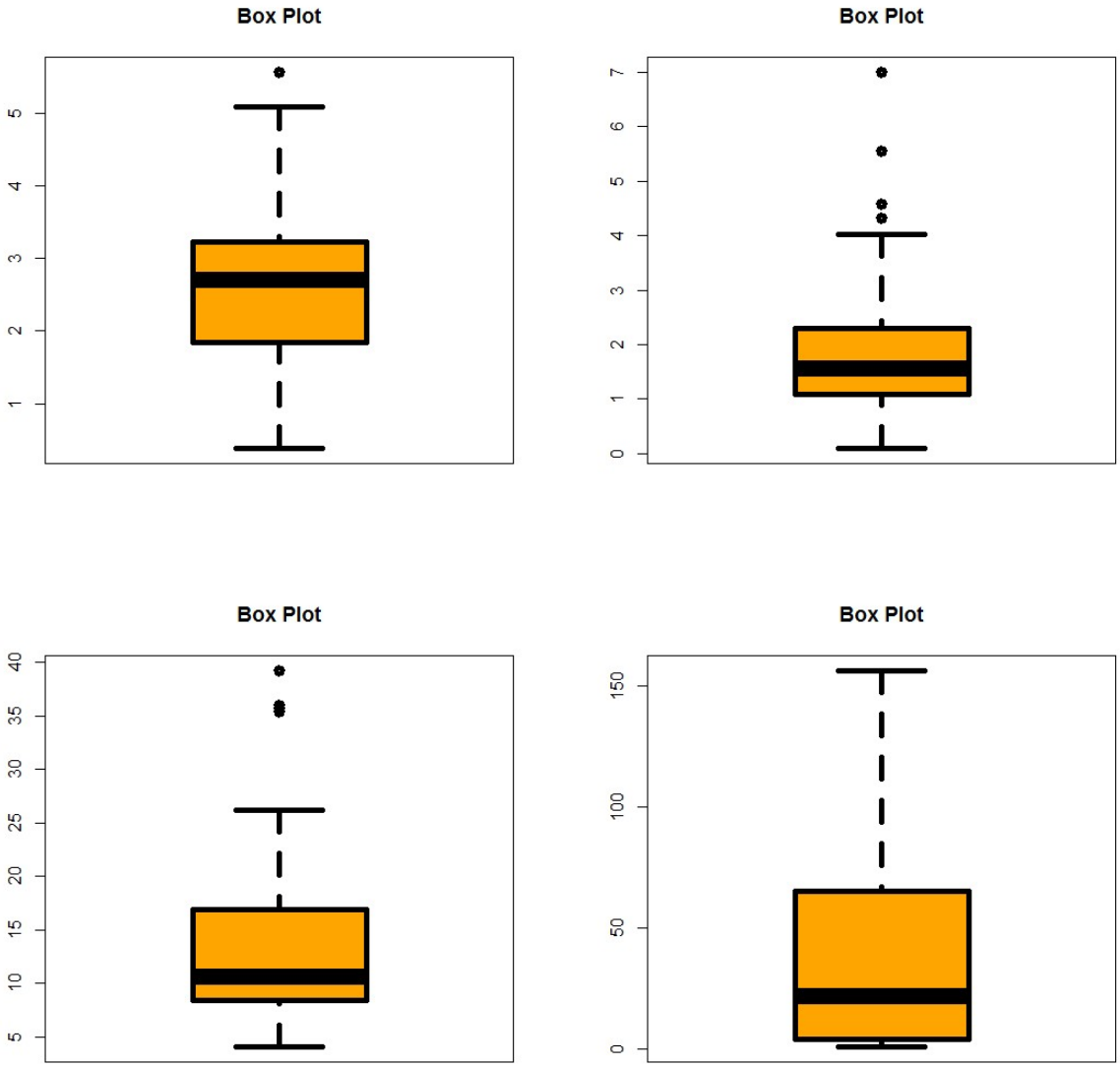

Figure 7. Box plots.

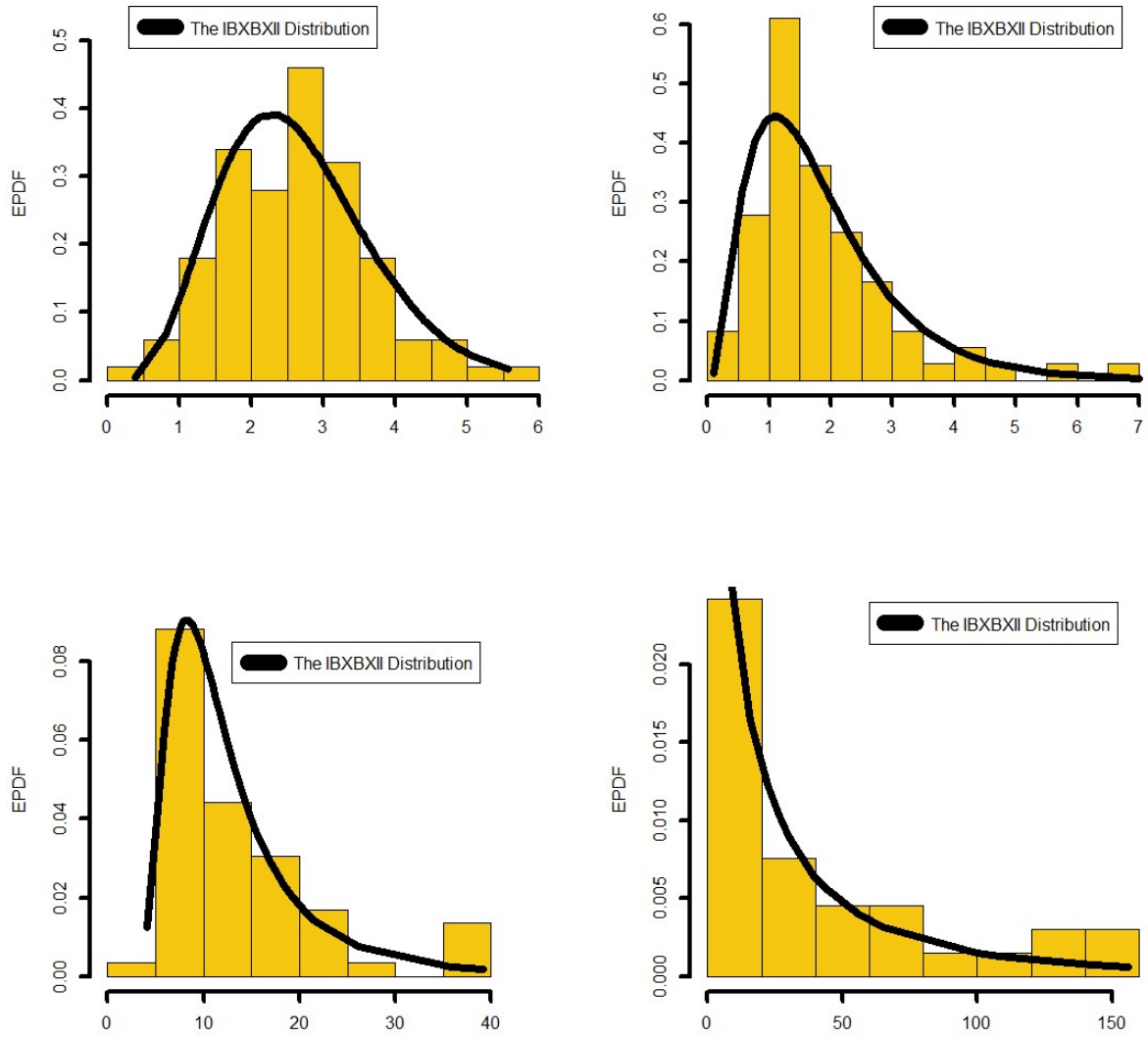

Figure 8. EPDF plots.

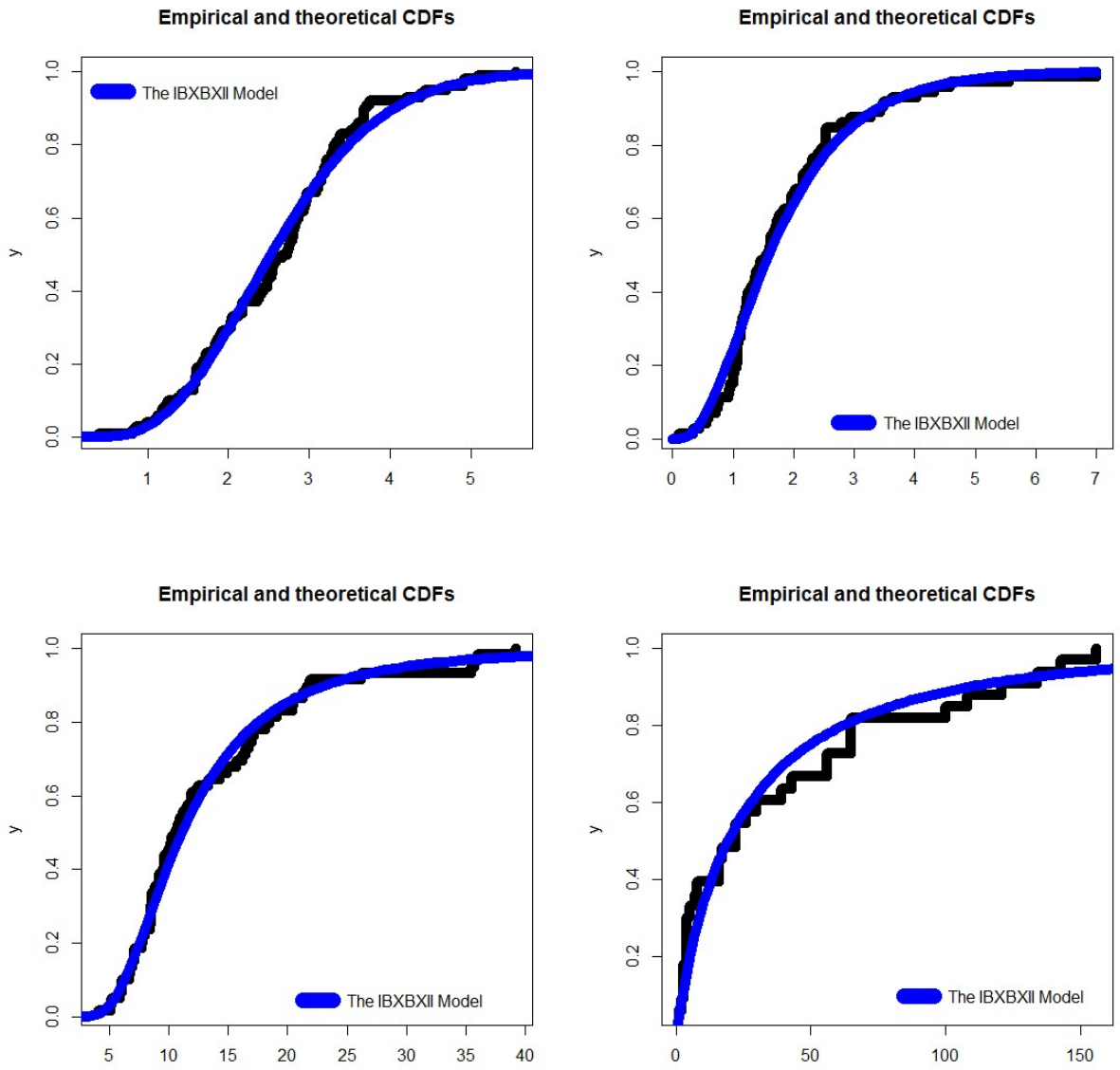

Figure 9. Empirical and theoretical CDFs.

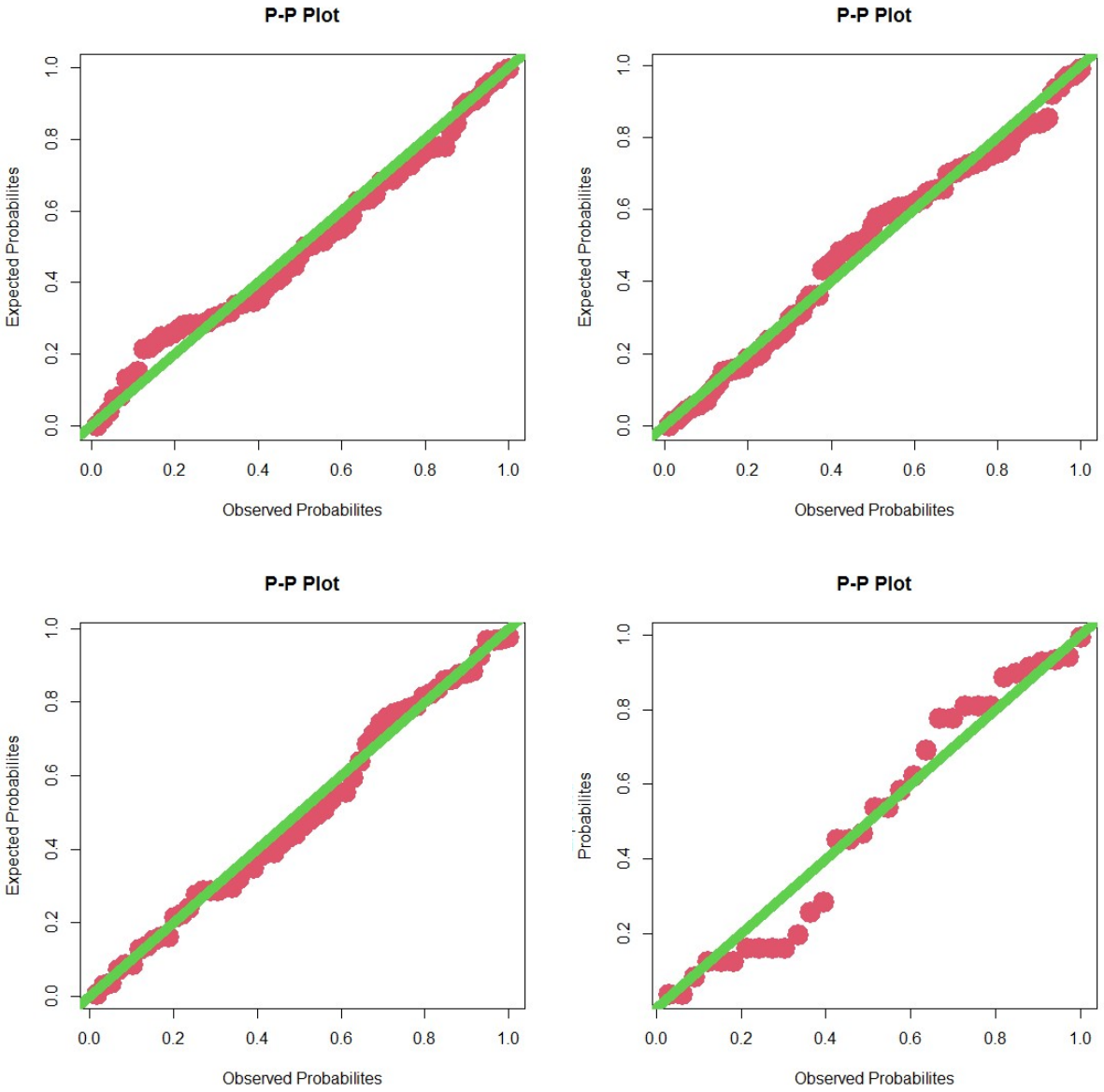

Figure 10. P-P plots.

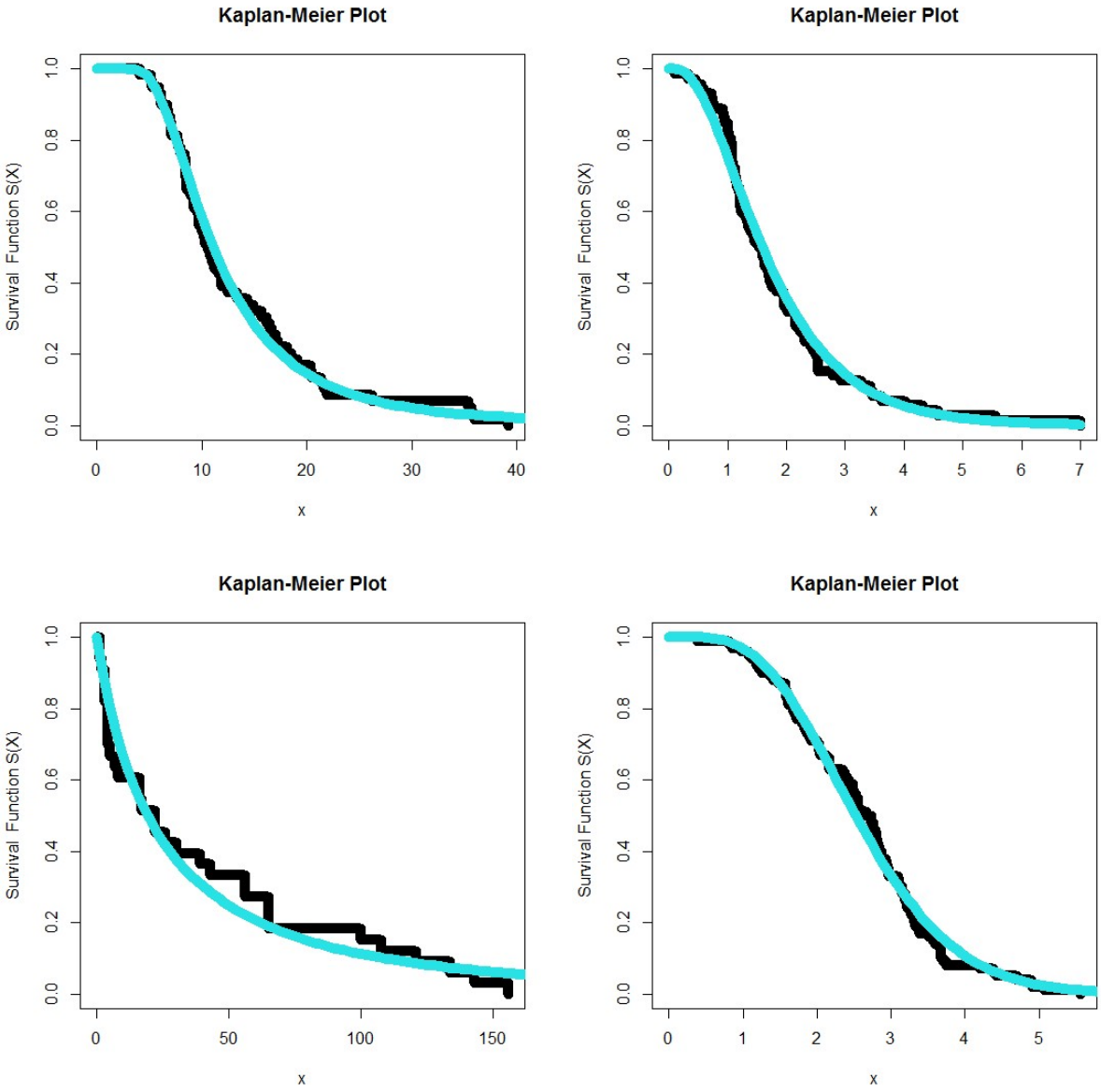

Figure 11. Kaplan-Meier survival plot.

Table 9 (the second column) gives the MLEs, SEs and CL values, respectively, for the data set I. Table 10 (the second column) shows the MLEs, SEs and CL values, respectively, for the data set II. Table 11 (the second column) presents the MLEs, SEs and CL values, respectively, for the data set III. Table 12 (the second column) provides the MLEs, SEs, and CL values, respectively, for the data set IV. Table 9 (the third column) presents the $\mathbb{C}_{\text{AI}}$, $\mathbb{C}_{\text{BYS}}$, $\mathbb{C}_{\text{HQ}}$ and $\mathbb{C}_{\text{CA}}$, Kolmogorov-Smirnov test (KS) and P-value (PV), respectively, for the data set I. Table 10 (the third column) shows the $\mathbb{C}_{\text{AI}}$, $\mathbb{C}_{\text{BYS}}$, $\mathbb{C}_{\text{HQ}}$ and $\mathbb{C}_{\text{CA}}$, KS and PV, respectively, for the data set II. Table 11 (the third column) gives the $\mathbb{C}_{\text{AI}}$, $\mathbb{C}_{\text{BYS}}$, $\mathbb{C}_{\text{HQ}}$ and $\mathbb{C}_{\text{CA}}$, KS and PV, respectively, for the data set III. Table 12 (the third column) shows the $\mathbb{C}_{\text{AI}}$, $\mathbb{C}_{\text{BYS}}$, $\mathbb{C}_{\text{HQ}}$ and $\mathbb{C}_{\text{CA}}$, KS and PV, respectively, for the data set IV. Based on the values in Tables 9–12, the IBXBXII model has the best fits as compared to BXII

extensions in the four applications with small values of $\mathbb{C}_{\text{AI}}$, $\mathbb{C}_{\text{BYS}}$, $\mathbb{C}_{\text{HQ}}$, $\mathbb{C}_{\text{CA}}$ and KS (and biggest corresponding PV) where for data set I $\mathbb{C}_{\text{AI}}$ =291.101, $\mathbb{C}_{\text{BYS}}$ =298.910, $\mathbb{C}_{\text{HQ}}$ =294.152, $\mathbb{C}_{\text{CA}}$ =291.121, KS =0.076266 and PV =0.6059. For data set II $\mathbb{C}_{\text{AI}}$ =205.242, $\mathbb{C}_{\text{BYS}}$ =212.102, $\mathbb{C}_{\text{HQ}}$ =208.888, $\mathbb{C}_{\text{CA}}$ =206.967, KS =0.10192 and PV =0.4431. For data set III $\mathbb{C}_{\text{AI}}$ =381.016, $\mathbb{C}_{\text{BYS}}$ =387.076, $\mathbb{C}_{\text{HQ}}$ =382.985, $\mathbb{C}_{\text{CA}}$ =384.667, KS =0.065129 and PV =0.9638. Finally for data set IV $\mathbb{C}_{\text{AI}}$ =310.001, $\mathbb{C}_{\text{BYS}}$ =315.323, $\mathbb{C}_{\text{HQ}}$ =311.201, $\mathbb{C}_{\text{CA}}$ =312.901, KS =0.14037 and PV =0.5339.

Table 9. Comparing the competing models under the data set I.

Competing Models	$\widehat{\zeta}, \widehat{\alpha_1}, \widehat{\alpha_2}, \widehat{\alpha}, \widehat{\beta}$	$C_{\text{AI}}, C_{\text{BYS}}, C_{\text{CA}}, C_{\text{HQ}}, KS, PV$
BXII	—, 5.9415, 0.1876, —	382.943, 388.125, 383.062, 385.052,0.1198,0.4446
	—, (1.2792) ,(0.0442), —	
MARBXII	—, 1.1923,4.8343,838.731, —	305.782, 313.681, 306.093, 308.966,0.08819,0.5698
	—, (0.9524),(4.8965),(229.347), —	
TOLBXII	—, 1.3503,1.0612,13.7228, —	323.542, 331.35, 323.772, 326.708,0.1037,0.4598
	—, (0.3782) ,(0.3837) ,(8.4003), —	
KMBXII	48.1034 ,79.5116 ,0.351 ,2.7340, —	303.764, 314.250, 304.182, 308.010,0.08990,0.5957
	(19.3481) ,(58.182) ,(0.093) ,(1.0763) , —	
BTBXII	359.6834 ,260.094 ,0.1753 ,1.1235 , —	305.642, 316.036, 306.061, 309.853,0.08733,0.5543
	(57.943) ,(132.203),(0.0132),(0.2433), —	
BEXBXII	0.3831, 11.944, 0.9375, 33.4021, 1.7053	305.822, 318.844, 306.433, 311.091,0.08609,0.5509
	(0.073), (4.634), (0.264), (6.281),(0.474)	
FBBXII	0.4214, 0.8354, 6.1115, 1.6746, 3.4505	304.264, 317.314, 304.892, 309.536,0.08436,0.5777
	(0.02), (0.944), (2.316), (0.227), (1.960)	
FKMBXII	0.5427,4.2237, 5.3137, 0.4116, 4.1527	305.530, 318.552, 306.144, 310.803,0.08743,0.5554
	(0.132), (1.884), (2.316), (0.495), (1.993)	
ZOBBXII	123.1443,0.3632, 139.2447, —, —	302.963, 310.718, 303.251, 306.134,0.09064,0.5815
	(243.03), (0.3435), (318.551), —, —	
IBXBXII	1564.531, 0.2255, 0.3834, —, —	291.101, 298.910, 291.121, 294.152,0.076266,0.6059
	(8.1451), (0.00248), (0.00962), —, —	

Table 10. Comparing the competing models under the data set II.

Competing Models	$\widehat{\zeta}, \widehat{\alpha_1}, \widehat{\alpha_2}, \widehat{\alpha}, \widehat{\beta}$	$C_{\mathrm{AI}}, C_{\mathrm{BYS}}, C_{\mathrm{CA}}, C_{\mathrm{HQ}}, KS, PV$
BXII	—, 3.1027, 0.4656, —, —	209.602, 214.135, 209.772, 211.4010.1443,0.3921
	—, (0.5383), (0.0772), —, —	
MARBXII	—, 2.2593,1.5343, 6.7605, —	209.743, 216.564, 210.093, 212.4420.1236,0.428
	—, (0.8643), (0.9074), (4.5872), —	
TOLBXII	—, 2.3934,0.4518,1.7967, —	211.803, 218.633, 212.132, 214.5220.1399,0.3999
	—, (0.9071), (0.2444),(0.9156), —	
KMBXII	14.103,7.426, 0.5256, 2.2746, —	208.763, 217.862, 209.363, 212.318,0.1443,0.4008
	(10.803), (11.851), (0.2702),(0.993), —	
BTBXII	2.5557, 6.0585,1.8076,0.29465, —	210.443, 219.543, 211.033, 214.062,0.1341,0.4102
	(1.8588), (10.3909), (0.9551),(0.4663), —	
BEXBXII	1.8755, 2.9910, 1.7803, 1.3414, 0.5716	212.10, 223.50, 213.020, 216.603,0.1443,0.3988
	(0.090), (1.711), (0.722), (0.812), (0.324)	
FBBXII	0.6217, 0.5496, 3.8386, 1.3817, 1.6656	206.803, 218.202, 207.731, 211.310,0.1332,0.4333
	(0.543), (1.010), (2.781), (2.313), (0.435)	
FKMBXII	0.5577, 0.3084, 3.992, 2.1314, 1.4754	206.503, 217.940, 207.414, 211.002,0.1212,0.4302
	(0.441), (0.311), (2.083), (1.836), (0.366)	
IBXBXII	314.671, 0.17453, 0.46435, —, —	205.242, 212.102, 206.967, 208.888,0.1019,0.4431
	1.0877, 0.03459, 0.039101, —, —	

Table 11. Comparing the competing models under the data set III.

Competing Models	$\widehat{\zeta}, \widehat{\alpha_1}, \widehat{\alpha_2}, \widehat{\alpha}, \widehat{\beta}$	$C_{\mathrm{AI}}, C_{\mathrm{BYS}}, C_{\mathrm{CA}}, C_{\mathrm{HQ}}, KS, PV$
BXII	—, 5.61548, 0.07243, —, —	518.426, 522.642, 518.467, 520.084,0.15959,0.61871
	—, (15.0466), (0.1945), —, —	
MARBXII	—, 8.0172, 0.4188, 70.3579, —	387.222, 389.38, 387.626, 389.68,0.069958,0.8654
	—, (22.0836), (0.3132), (63.8311), —	
TOLBXII	—, 91.324, 0.0127, 141.0737, —	385.944, 392.184, 386.384, 388.403,0.069437,0.9301
	—, (15.071), (0.0024), (70.0287), —	
KMBXII	18.137, 6.854, 10.697, 0.0867, —	385.583, 393.940, 386.312, 388.836,0.06823,0.9242
	(3.611), (1.034), (1.164), (0.0125), —	
BTBXII	26.7256, 9.7555, 27.3639, 0.0210, —	385.563, 394.103, 386.340, 389.104,0.06837,0.9239
	(9.472), (2.718), (12.353), (0.006), —	
BEXBXII	2.9245, 2.914, 3.274, 12.485, 0.372	387.044, 397.424, 388.174, 391.09,0.069655,0.9111
	(0.546), (0.555), (1.249), (6.888), (0.77)	
FBBXII	30.447, 0.587, 1.086, 5.168, 7.8626	386.742, 397.144, 387.827, 390.84,0.06811,0.9054
	(91.74), (1.01), (1.025), (8.26), (15.02)	
FKMBXII	12.8784, 1.2255, 1.6615, 1.4112, 3.7324	386.962, 397.326, 388.019, 391.062,0.06854,0.9054
	(3.421), (0.1315), (0.032), (0.15), (1.11)	
IBXBXII	5.37643, 1.44954, 0.14449, —, —	381.016, 387.076, 382.985, 384.667,0.065129,0.9638
	0.62791, 1.4225, 0.12549, —, —	

Table 12. Comparing the competing models under the data set IV.

Competing Models	$\widehat{\zeta}, \widehat{\alpha_1}, \widehat{\alpha_2}, \widehat{\alpha}, \widehat{\beta}$	$C_{\mathrm{AI}}, C_{\mathrm{BYS}}, C_{\mathrm{CA}}, C_{\mathrm{HQ}}, KS, PV$
BXII	—, 58.723,0.0064, —, —	328.201, 331.139, 328.601, 329.191,0.1300,0.4876
	—, (42.383), (0.0044), —, —	
MARBXII	—, 11.8321, 0.0777, 12.2541, —	315.543, 320.011, 316.373, 317.044,0.1366,0.5043
	—, (4.3686), (0.015), (7.776), —	
TOLBXII	—,0.2814, 1.8834 ,50.2166, —	316.261, 320.732, 317.049, 317.763,0.1366,0.5121
	—, (0.2884), (2.4024), (176.54), —	
KMBXII	9.2014, 36.4254, 0.2411,0.9421, —	317.363, 323.303, 318.719, 319.343,0.1355,5066
	(10.052), (35.652), (0.1645), (1.0432), —	
BTBXII	96.104, 52.121, 0.104, 1.227, —	316.462, 322.405, 317.829, 318.422,0.1372,0.5133
	(41.201), (33.490), (0.023), (0.326), —	
BEXBXII	0.08214, 5.0324, 1.5317, 31.2523, 0.3122	317.58, 325.064, 319.804, 320.095,0.1350,0.5054
	(0.071), (3.852), (0.0124), (12.943), (0.032)	
FBBXII	15.1943, 32.0477, 0.2313, 0.5814, 21.851	317.826, 325.342, 320.089, 320.363,0.1341,0.5021
	(11.601), (9.8721), (0.093), (0.073), (35.2)	
FKMBXII	14.7322, 15.2815, 0.2934, 0.8392, 0.0344	317.736, 325.212, 319.918, 320.262,0.1374,0.5000
	(12.366), (18.871), (0.222), (0.854), (0.082)	
DBXII	251.2325, 0.08153, 0.42013, —, —	310.001, 315.323, 311.201, 312.901,0.14037,0.5339
	2.3291, 0.0363, 0.050710, —, —	

7. Two actuarial case studies

Risk analysis plays a crucial role in managing bimodal insurance claims data, offering assistance to insurance companies and risk managers in navigating the unique challenges presented by this distribution. Bimodal distributions in such data often stem from distinct groups of claims, such as low-frequency high-severity and high-frequency low-severity claims. The Value at Risk (VaR) indicator holds particular significance in this scenario, as it quantifies potential losses within a specified confidence interval, providing insights into adverse market movements or events. The presence of fat tails in bimodal insurance claims data suggests a heightened likelihood of extreme events, and VaR analysis aids insurers in quantifying and managing associated risks by offering valuable information on the size and frequency of extreme losses. In this Section, we consider new actuarial data sets, the first one is a new bimodal insurance claims data set and the second referred as the insurance revenue data (*see https://data.world/data sets/insurance*). These insurance claims data have been described graphically in Figures 12 and 13. Figure 12 gives the Cullen and Frey plot, nonparametric kernel density estimation plot, TTT, and box plots under the bimodal insurance-claims data set. Figure 13 gives the Q-Q plot plot, Scatter plot, the autocorrelation function (ACF) plot, and the partial autocorrelation function (partial ACF) plot under the the bimodal insurance-claims data set.

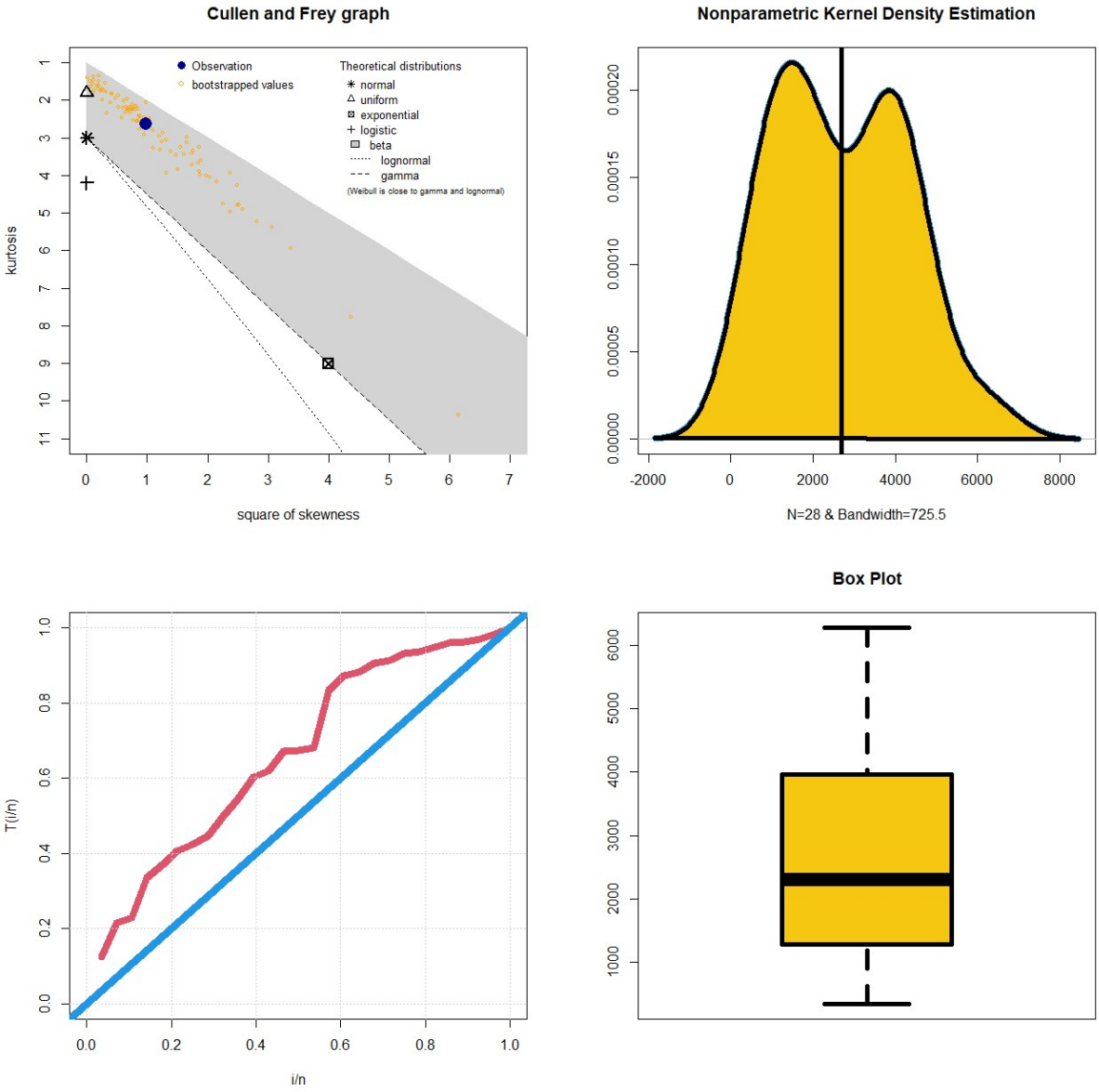

Figure 12. The Cullen and Frey plot, nonparametric kernel density estimation plot, TTT and box plots under the the bimodal insurance-claims data set.

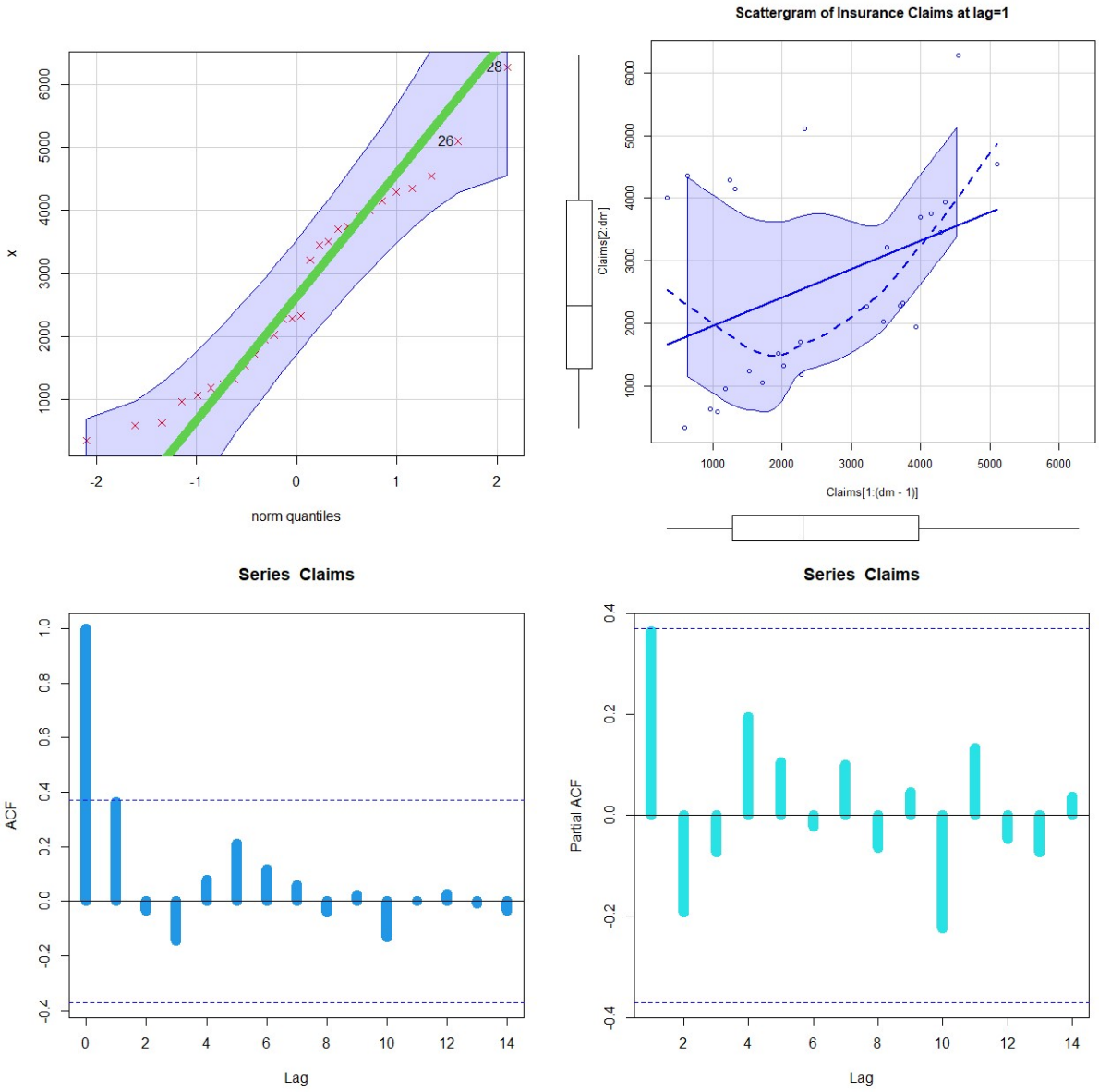

Figure 13. The Q-Q plot, Scatter plot, the ACF plot and the partial ACF plot under the bimodal insurance-claims data set.

Figure 12 (the top left panel) gives the Cullen and Frey plot under the insurance-claims data set. Due to the Cullen and Frey plot, it is seen that the insurance-claims data set does not follow any of the mentioned distributions. Figure 12 (the top right panel) gives the nonparametric kernel density estimation plot under the bimodal insurance-claims data set. According to the nonparametric kernel density estimation plot it is seen that the insurance-claims data set is a bimodal data. Figure 12 (the bottom left panel) gives the TTT plot under the bimodal insurance-claims data set. Due to Figure 12 (the bottom left panel), the TTT plot under the bimodal insurance-claims data set indicates that the bimodal insurance-claims data set has an increasing HRF. Figure 12 (the bottom right panel) gives the box plot under the bimodal insurance-claims data set which indicates that the bimodal insurance-

claims data set has no extreme observations. Figure 13 (the top left panel) gives the Q-Q plot under the bimodal insurance-claims data set which indicates that the bimodal insurance-claims data set has no extreme observations. Figure 13 (the top right panel) gives the scatter plot under the bimodal insurance-claims data set. Figure 13 (the bottom left panel) gives the ACF plot under the bimodal insurance-claims data set. The partial autocorrelation function (partial ACF) plot is a graphical representation used in time series analysis to understand the relationship between a time series and its lagged values while controlling for intermediate lags. Figure 13 (the bottom right panel) gives the partial ACF plot under the bimodal insurance-claims data set. The insurance insurance-revenue data have been described graphically in Figures 14 and 15. Figure 14 gives the Cullen and Frey plot, nonparametric kernel density estimation plot, TTT, and box plots under the insurance-revenue data set. Figure 15 gives the Q-Q plot plot, Scatter plot, the ACF plot, and the partial ACF plot under the the insurance-revenue data set.

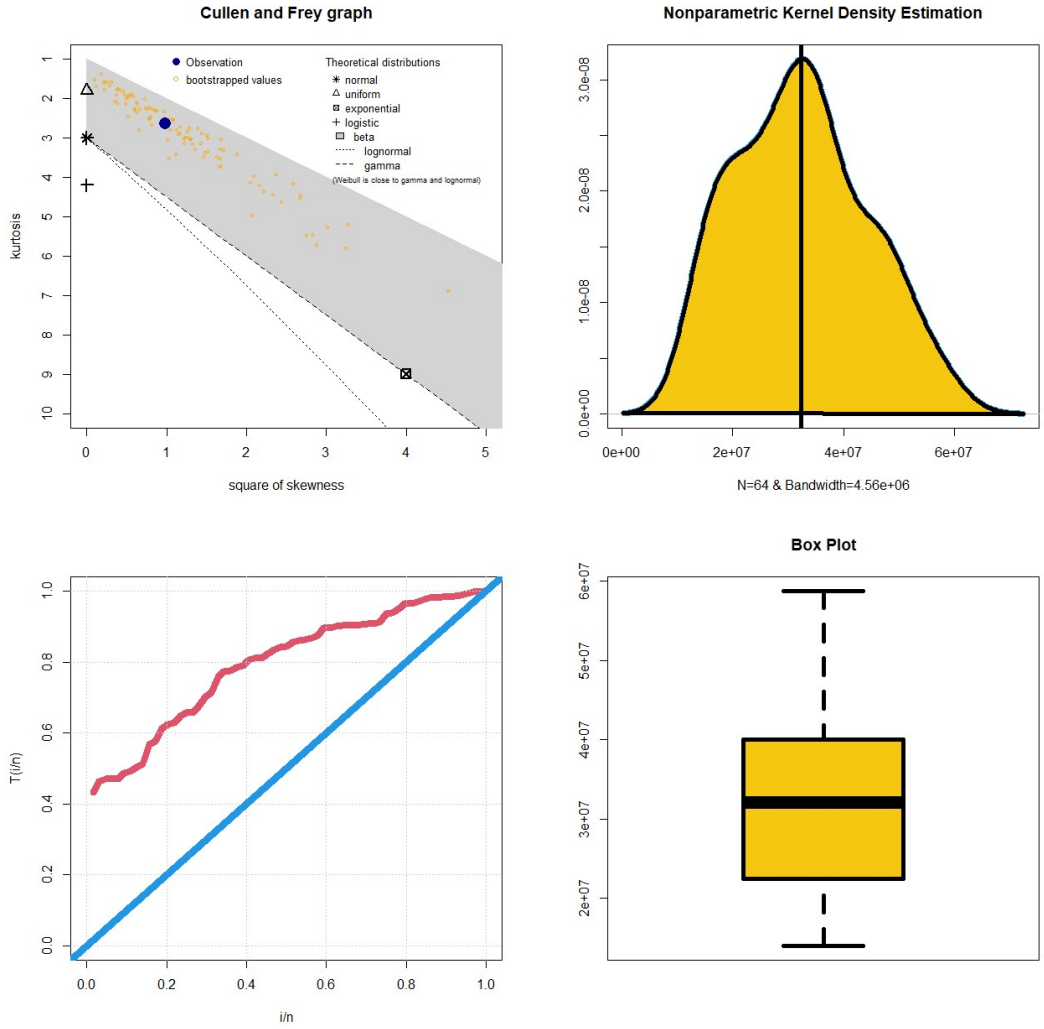

Figure 14. The Cullen and Frey plot, nonparametric kernel density estimation plot, TTT and box plots under the revenues data set.

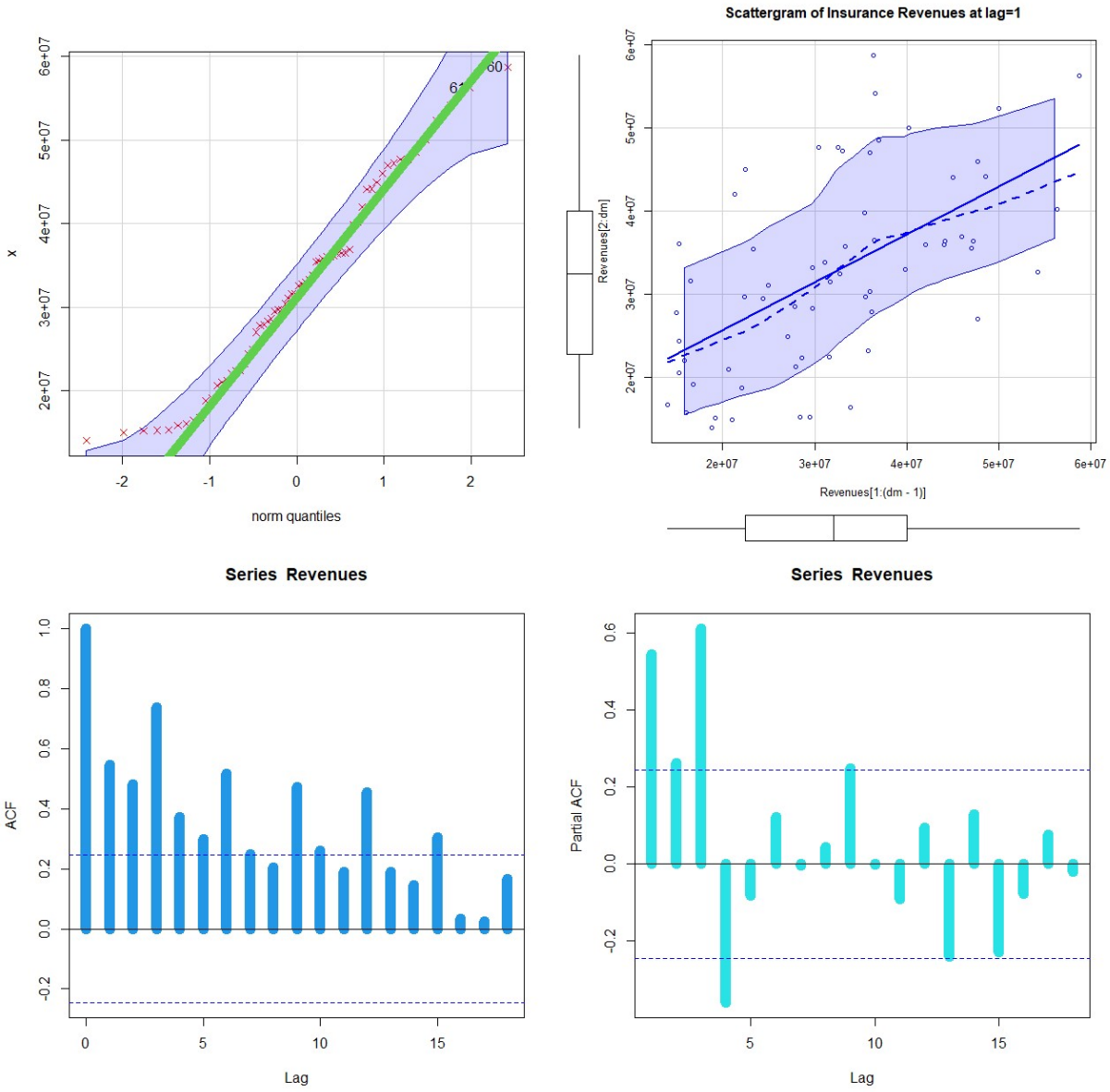

Figure 15. The Q-Q plot, Scatter plot, the ACF plot and the partial ACF plot under the revenue data set.

Figure 14 (the top left panel) gives the Cullen and Frey plot under the insurance-revenue data set. Due to the Cullen and Frey plot, it is seen that the insurance-revenue data set does not follow any of the mentioned distributions. Figure 14 (the top right panel) gives the nonparametric kernel density estimation plot under the insurance-revenue data set. According to the nonparametric kernel density estimation plot it is seen that the insurance revenue is semi-symmetric data. Figure 14 (the bottom left panel) gives the TTT plot under the insurance-revenue data set. Due to Figure 14 (the bottom left panel), the TTT plot under the insurance-revenue data set indicates that the insurance-revenue data set has an increasing HRF. Figure 14 (the bottom right panel) gives the box plot under the insurance-revenue data set which indicates that the insurance-revenue data set has no extreme observations.

Figure 15 (the top left panel) gives the Q-Q plot under the insurance-revenue data set which indicates that the insurance-revenues data set has no extreme observations. Figure 15 (the top right panel) gives the scatter plot under the insurance-revenue data set. The primary function of the ACF plot is to visualize the serial correlation or autocorrelation in a time series. Figure 15 (the bottom left panel) gives the ACF plot under the insurance-revenue data set. Figure 15 (the bottom right panel) gives the partial ACF plot under the insurance-revenue data set. In addition to the graphical analysis previously presented, we can describe the data numerically by providing a numerical summary of the insurance data used in actuarial risk analysis. Table 13 gives a summary of the two insurance data.

Table 13. Numerical description for the two actuarial data sets.

Summery↓ & Data→	Claims	Revenue
Mean	2702.572	32360452
SD	1569.656	11641499
Skewness	0.2986363	0.2668196
Kurtosis	2.144497	2.264141
Max and Min	6283.001, 340.0001	58756474, 14021480
Median	2298.999	32090875
Length	28	64
Quantile (0.33%, 0.66%)	1694.9008, 3667.6184	27628461, 36090317
Quantile (0.25%, 0.75%)	1299.4998, 3949.2490	22426547, 39929985

Table 14 provides the risk analysis under the actuarial claims data set, where q =75%, 80%, 85%, 90%, 95%, 99% and 99.5%. Moreover, the MOOP $\mathbb{V}_1|P = 2$ are estimated under q =75%, 80%, 85%, 90%, 95%, 99% and 99.5%. Under actuarial claims data it is seen that:

(1) The $\mathbb{V}_1$ indicator increases as q increases, it started with $4.129296|q = 75\%$ ended with $513.1953 - |q = 99.5\%$, where

$$\mathbb{V}_1|q = 75\% < \mathbb{V}_1|q = 80\% < ... < \mathbb{V}_1|q = 99.5\%.$$

(2) The $\mathbb{V}_2$ indicator increases as q increases, it started with $13.30721|q = 75\%$ ended with $1052.658-|q = 99.5\%$, where

$$\mathbb{V}_2|q = 75\% < \mathbb{V}_2|q = 80\% < ... < \mathbb{V}_2|q = 99.5\%.$$

(3) The $\mathbb{V}_3$ indicator decreases as q increases, it started with $3.820954|q = 75\%$ ended with $3.663571-|q = 95\%$, then the $\mathbb{V}_3$ indicator increases as q increases, it started with $5.879942|q = 75\%$ ended with $13087.82|q = 99.5\%$, where

$$\mathbb{V}_3|q = 75\% > \mathbb{V}_3|q = 80\% > ... > \mathbb{V}_3|q = 95\% < \mathbb{V}_3|q = 99\% < \mathbb{V}_3|q = 99.5\%.$$

(4) The $\mathbb{V}_4$ indicator increases as q increases, where

$$\mathbb{V}_4|q = 75\% < \mathbb{V}_4|q = 80\% < ... < \mathbb{V}_4|q = 99.5\%.$$

(5) The $e(\mathbb{V}_1)$ indicator decreases as q increases, where

$$e(\mathbb{V}_1)|q = 75\% > e(\mathbb{V}_1)|q = 80\% > ... > e(\mathbb{V}_1)|q = 99.5\%.$$

(6) The MOOP $\mathbb{V}_1|P = 2 > \mathbb{V}_1 \ \forall \ q|q$ =75%, 80%, 85%, 90%, 95%, 99% and 99.5%.

Table 14. Risk analysis under the actuarial claims data set.

q	$\mathbb{V}_1$	$\mathbb{V}_2$	$\mathbb{V}_3$	$\mathbb{V}_4$	$e(\mathbb{V}_1)$	MOOP $\mathbb{V}_1\|P = 2$
75%	4.129296	13.30721	3.820954	44.46739	3.222634	9.3921611
80%	6.657118	21.37147	3.773506	70.61630	3.210319	15.767623
85%	9.342134	29.87662	3.737976	97.88235	3.198051	23.449813
90%	15.06109	47.79871	3.691046	154.8284	3.173656	29.980094
95%	34.07426	105.6841	3.663571	340.0352	3.101582	43.710911
99%	226.8363	585.4409	5.879942	2883.492	2.580896	456.88933
99.5%	513.1953	1052.658	16.45130	13087.82	2.051183	888.98398

Table 15 provides the risk analysis under the actuarial revenues data set, where q =75%, 80%, 85%, 90%, 95%, 99% and 99.5%. Moreover, the MOOP $\mathbb{V}_1|P = 2$ are estimated under q =75%, 80%, 85%, 90%, 95%, 99% and 99.5%. Under actuarial revenues data it is seen that:

(1) The $\mathbb{V}_1$ indicator increases as q increases, it started with $72.74761|q = 75\%$ ended with $1134.023-|q = 99.5\%$, where

$$\mathbb{V}_1|q = 75\% < \mathbb{V}_1|q = 80\% < ... < \mathbb{V}_1|q = 99.5\%.$$

(2) The $\mathbb{V}_2$ indicator increases as q increases, it started with $248.409|q = 75\%$ ended with $304.2253|q = 99.5\%$, where

$$\mathbb{V}_2|q = 75\% < \mathbb{V}_2|q = 80\% < ... < \mathbb{V}_2|q = 99.5\%.$$

(3) The $\mathbb{V}_3$ indicator decreases as q increases, it started with $213.2133|q = 75\%$ ended with $2786784|q = 99.5\%$, where

$$\mathbb{V}_3|q = 75\% < \mathbb{V}_3|q = 80\% < ... < \mathbb{V}_3|q = 99.5\%.$$

(4) The $\mathbb{V}_4$ indicator increases as q increases, where

$$\mathbb{V}_4|q = 75\% < \mathbb{V}_4|q = 80\% < ... < \mathbb{V}_4|q = 99.5\%.$$

(5) The $e(\mathbb{V}_1)$ indicator decreases as q increases, where

$$e(\mathbb{V}_1)|q = 75\% > e(\mathbb{V}_1)|q = 80\% > ... > e(\mathbb{V}_1)|q = 99.5\%.$$

(6) The MOOP $\mathbb{V}_1|P = 2 > \mathbb{V}_1 \ \forall \ q|q$ =75%, 80%, 85%, 90%, 95%, 99% and 99.5%.

Table 15. Risk analysis under the actuarial revenues data set.

q	$\mathbb{V}_1$	$\mathbb{V}_2$	$\mathbb{V}_3$	$\mathbb{V}_4$	$e(\mathbb{V}_1)$	MOOP $\mathbb{V}_1\|P=2$
75%	72.74761	248.409	213.2133	30981.341	3.414669	102.761889
80%	136.3578	323.7453	712.8563	119648.02	2.374235	152.710913
85%	411.5226	393.8717	23278.87	3354443.5	0.9571083	604.810914
90%	423.1799	393.6161	26062.26	3710938.9	0.930139	664.909612
95%	435.3047	393.2293	29252.05	4113263.1	0.9033427	670.109439
99%	461.0562	392.0397	37140.02	5083795.7	0.8503079	716.221348
99.5%	1134.023	304.2253	2786784	192215514	0.2682709	1587.87301

8. Assessing the MOOP value at risk under the IBXBXII model

In the realm of risk assessment, the proposed distribution's performance is evaluated by comparing its distribution function to the Mean of Order-P (MOOP). This comparison is driven by the goal of assessing the distribution's effectiveness, especially in finance-related applications such as risk estimation and extreme occurrences.

In this portion, we run a numerical simulation study to evaluate the performance of the estimators of MOOP $\mathbb{V}_1$ based on the QF of the of the IBXBXII model and that of the methodology of the MOOP. Specifically, we are interested in determining whether or whether the MOOP methodology produces more accurate results. We generate samples of size n ($n = 50, 150, 300$ and 500) from the new IBXBXII model with parameters ζ, α_1 and α_2 such that both negatively and positively skewed PDFs are obtained for assessing the estimators and their performance. Furthermore, to assess the adaptability of the suggested distribution, we generate sample data by simulating observations from the widely recognized BXII distribution, which is characterized by the following survival function with parameters α_1 and α_2:

$$S_{\alpha_1,\alpha_2}(z)|_{(z\geq 0)} = (1 + z^{\alpha_2})^{-\alpha_1}$$

In this scenario, we make a conscientious choice about the shape parameter in order to accomplish both a negative and a positive skewness. Because we have made this selection, we are able to test the performance of the estimators under a variety of skewness circumstances. To determine the absolute bias (ABS) and mean squared errors (MSEs) for every estimator, we run every simulation scenario several times (where N is larger than or equal to 1000 times), and then produce multiple repeats of those runs. To be more specific, we use the maximum likelihood technique for estimating purposes when dealing with the IBXBXII distribution. In spite of this, when it comes to the MOOP value at risk estimator, which is comparable to any semi-parametric estimator in extreme value statistics, the selection of the parameter k, which reflects the number of top order statistics, becomes extremely critical. This choice has an immediate and direct influence on both the bias and the variance, particularly in respect to the tail index and, as a result, the high quantile (or value at risk). In addition, for this specific estimator, an additional crucial consideration that arises regards the selection of the parameter P.

The outcomes of our simulation study are presented in Tables 16–21. Tables 16–18 correspond to the negatively skewed distributions, where we selected the value of the parameter as follows: ($\zeta = 150$, $\alpha_1 = 2$, $\alpha_2 = 5$; $\zeta = 50$, $\alpha_1 = 3$, $\alpha_2 = 2$; $\zeta = 200$, $\alpha_1 = 3$, $\alpha_2 = 2$). In those cases, it is noted

that the $S(Z) = -0.1336004, -0.1492178, -0.5236663$ respectively. While Tables 19–21 pertain to the positively skewed distributions when the samples are generated from the IBXBXII distribution, where we selected the value of the parameter as follows: $(\zeta = 1, \alpha_1 = 3, \alpha_2 = 2; \zeta = 20, \alpha_1 = 3, \alpha_2 = 2; \zeta = 3, \alpha_1 = 1, \alpha_2 = 5)$. In those cases, it is noted that the $S(Z)$ =1.6074570, 0.0320100, 1.308430 respectively. The results are reported for various quantile values, specifically 95%, 95% and 99.5%, across different sample sizes.

Regarding the data that are skewed in a negative direction (see Tables 16–21). Tables 16–18 show that the MOOP estimate for $\mathbb{V}_1$ performs significantly better than the suggested IBXBXII model estimator. In contrast, the MOOP estimator for indicator V1 is not superior to the suggested IBXBXII model estimate when applied to data with a positively skewed distribution. The results of the regressions and the average square errors both make it abundantly evident that the IBXBXII distribution has a strong tail to the right. This is the conclusion that can be drawn from the information presented here. In other words, the new distribution can be deemed more appropriate when the insurance data is skewed to the right or has a long tail to the right. This is because both of these characteristics indicate that the right side of the distribution is more prominent. It is important to point out that the outcomes of the simulation trials revealed that the new distribution is suitable for mathematical modeling and actuarial risk analysis in general. In a general sense, we are able to emphasize the following primary results:

(1) MSE for the MOOP estimator for indicator $\mathbb{V}_1$ decreases as q increases.

(2) MSE for the MOOP estimator for indicator $\mathbb{V}_1$ < MSE for the IBXBXII estimator for indicator $\mathbb{V}_1$ for all negative simulated data.

(3) MSE for the IBXBXII estimator for indicator $\mathbb{V}_1$ decreases as q increases.

(4) ABS for the MOOP estimator for indicator $\mathbb{V}_1$ < ABS for the IBXBXII estimator for indicator $\mathbb{V}_1$ for all negative simulated data.

(5) MSE for the MOOP estimator for indicator $\mathbb{V}_1$ > MSE for the IBXBXII estimator for indicator $\mathbb{V}_1$ for all positive simulated data.

(6) ABS for the MOOP estimator for indicator $\mathbb{V}_1$ < ABS for the IBXBXII estimator for indicator $\mathbb{V}_1$ for all positive simulated data.

(7) For $n = 500$, the results of the MSE for the MOOP estimator for indicator $\mathbb{V}_1$ get very close to the MSE for the IBXBXII estimator for indicator $\mathbb{V}_1$ for all simulated data.

Nevertheless, regardless of whether the data are skewed to the right or the left, it is possible to assert that the IBXBXII distribution meets the criteria for a competitive distribution when applied to a sizeable sample. The fact that the bias and MSE of the estimators decreases as the sample size increases is an indication of the empirical consistency of the estimators in general. This is true for each and every circumstance that is taken into consideration. In addition to this, the IBXBXII model provides an estimator of the indicator $\mathbb{V}_1$ that has both less of a bias and a smaller MSE value than other estimators. Therefore, it is possible to consider the recommended estimator to be suitable for the purpose of estimating indicator $\mathbb{V}_1$ in the event that the underlying distribution is either positively or

negatively skewed. This is because the effect of using the suggested estimator is that the indicator can be estimated.

Table 16. ABS and MSE under MOOP and IBXBXII with $q = 0.95, \zeta = 150, \alpha_1 = 2, \alpha_2 = 5$.

	ABS		MSE	
$n\|q = 95\%$	IBXBXII	MOOP	IBXBXII	MOOP
50	0.291323	0.002853	0.330868	0.083215
150	0.194507	0.011421	0.133234	0.010731
300	0.014406	0.003134	0.092030	0.002030
500	0.003816	0.000925	0.010032	0.000939
$n\|q = 99\%$				
50	0.110880	0.012022	0.690910	0.900028
150	0.023221	0.008940	0.556034	0.602821
300	0.005154	0.006781	0.301054	0.321487
500	0.000440	0.004343	0.100090	0.011344
$n\|q = 99.5\%$				
50	0.010091	0.008000	0.996891	0.800321
150	0.048500	0.007124	0.676731	0.742865
300	0.004111	0.006612	0.225555	0.420459
500	0.000390	0.003333	0.109092	0.010310

Table 17. ABS and MSE under MOOP and IBXBXII with $q = 0.95, \zeta = 50, \alpha_1 = 3, \alpha_2 = 2$.

	ABS		MSE	
$n\|q = 95\%$	IBXBXII	MOOP	IBXBXII	MOOP
50	0.278712	0.033333	0.879813	0.111981
150	0.194652	0.011219	0.776574	0.101098
300	0.167781	0.006999	0.534332	0.001919
500	0.100761	0.000210	0.276732	0.001111
$n\|q = 99\%$				
50	0.918434	0.301121	0.924379	0.191466
150	0.400680	0.215133	0.194303	0.131043
300	0.105555	0.210149	0.033123	0.041953
500	0.006001	0.010531	0.030540	0.012522
$n\|q = 99.5\%$				
50	0.978434	0.569832	0.990325	0.391466
150	0.404682	0.515433	0.175433	0.271043
300	0.160093	0.300693	0.100120	0.099009
500	0.016090	0.010532	0.006254	0.001558

Table 18. ABS and MSE under MOOP and IBXBXII with $q = 0.95, \zeta = 200, \alpha_1 = 3, \alpha_2 = 2$.

	ABS		MSE	
$n\|q = 95\%$	IBXBXII	MOOP	IBXBXII	MOOP
50	0.299999	0.154981	0.176763	0.331323
150	0.149920	0.101034	0.555573	0.204315
300	0.197819	0.100913	0.313212	0.109103
500	0.006432	0.014315	0.200124	0.000154
$n\|q = 99\%$				
50	0.129582	0.129811	0.156767	0.175454
150	0.111300	0.115934	0.087800	0.010777
300	0.003232	0.003659	0.007555	0.001716
500	0.008755	0.009149	0.005235	0.000666
$n\|q = 99.5\%$				
50	0.129554	0.199811	0.153255	0.183333
150	0.104687	0.125432	0.074321	0.091099
300	0.010213	0.100655	0.001708	0.001654
500	0.006323	0.004343	0.005255	0.000931

Table 19. ABS and MSE under MOOP and IBXBXII with $q = 0.95, \zeta = 1, \alpha_1 = 3, \alpha_2 = 2$.

	ABS		MSE	
$n\|q = 95\%$	IBXBXII	MOOP	IBXBXII	MOOP
50	0.201392	0.354001	0.168891	0.313668
150	0.143245	0.301054	0.105521	0.214322
300	0.014312	0.190014	0.313212	0.119102
500	0.000213	0.001332	0.100124	0.000159
$n\|q = 99.5\%$				
50	0.101644	0.104024	0.113338	0.355555
150	0.040434	0.100029	0.105445	0.100004
300	0.046667	0.029044	0.098122	0.016121
500	0.000335	0.003333	0.000878	0.005026
$n\|q = 99.5\%$				
50	0.101432	0.100024	0.138812	0.212121
150	0.100787	0.031022	0.011111	0.146664
300	0.034301	0.009044	0.010243	0.100100
500	0.000214	0.003333	0.000077	0.000122

Table 20. ABS and MSE under MOOP and IBXBXII with $q = 0.95$, $\zeta = 20, \alpha_1 = 3, \alpha_2 = 2$.

	ABS		MSE	
$n\|q = 95\%$	IBXBXII	MOOP	IBXBXII	MOOP
50	0.043344	0.114055	0.188822	0.200362
150	0.041050	0.101022	0.100012	0.114312
300	0.000312	0.090014	0.113214	0.010108
500	0.000219	0.000420	0.000199	0.000051
$n\|q = 99.5\%$				
50	0.110991	0.112636	0.105144	0.112434
150	0.098229	0.111044	0.014171	0.051545
300	0.006364	0.005415	0.014111	0.001177
500	0.000646	0.000486	0.000609	0.000555
$n\|q = 99.5\%$				
50	0.100451	0.102645	0.100120	0.111885
150	0.080822	0.031002	0.015678	0.046545
300	0.002366	0.004048	0.013993	0.001095
500	0.000214	0.000982	0.000575	0.000425

Table 21. ABS and MSE under MOOP and IBXBXII with $q = 0.95$, $\zeta = 20, \alpha_1 = 3, \alpha_2 = 2$.

	ABS		MSE	
$n\|q = 95\%$	IBXBXII	MOOP	IBXBXII	MOOP
50	0.209354	0.200211	0.019899	0.100999
150	0.153993	0.141454	0.012878	0.076761
300	0.100024	0.050519	0.003003	0.002708
500	0.000334	0.000111	0.000043	0.000044
$n\|q = 99.5\%$				
50	0.102624	0.016951	0.100555	0.124343
150	0.043386	0.011043	0.013224	0.019543
300	0.003363	0.009434	0.005656	0.003111
500	0.000666	0.000765	0.000387	0.000222
$n\|q = 99.5\%$				
50	0.090043	0.013648	0.110109	0.099882
150	0.033383	0.008143	0.017854	0.008548
300	0.001364	0.007488	0.004343	0.002090
500	0.000032	0.000552	0.000331	0.000121

9. Conclusions

In-depth scrutiny is conducted on the inverse Burr-X Burr-XII (IBXBXII) distribution, tailored for asymmetric-bimodal loss data. This thorough investigation delves into various parameters, encompassing skewness, kurtosis, moments, and others, aligning with the paper's objectives focused

on analyzing the distinctive properties of this novel distribution. The IBXBXII distribution proves beneficial in three distinct scenarios, each serving a specific purpose. Firstly, the exploration centers on entropy investigation, evaluating four entropy models -Rényi entropy, Arimoto entropy, Tsallis entropy, and Havrda-Charvat entropy- via exhaustive analytical and numerical methods. A comparative study using the IBXBXII distribution further illustrates its utility. Secondly, the research underscores the significance of the new distribution and its applicability in mathematical, statistical, and applied modeling across diverse fields, including economics, engineering, dependability, and medicine. Through a meticulous comparison with alternative distributions commonly employed in applied modeling, the IBXBXII distribution emerges as the most suitable choice, supported by four real-world data applications demonstrating its favorable outcomes across various statistical tests. The third aspect focuses on employing the IBXBXII distribution in the examination of actuarial risks, particularly in scrutinizing probability distribution tails related to actuarial data. Case studies involving bimodal actuarial data pertinent to insurance claims and revenues are incorporated, utilizing five risk indicators to assess and calculate maximum potential losses.

Overall, the study provides a comprehensive exploration of the IBXBXII distribution, showcasing its adaptability and effectiveness in diverse analytical scenarios, including entropy analysis, field applications, and actuarial risk assessments.These indicators are used in the evaluation process. The five indicators are compared under the new model with the Mean of Order-P (MOOP $\mathbb{V}_1|P = 2$) methodology. The value at risk was numerically analyzed in each case using the five actuarial indicators and using varying levels of statistical confidence. A comprehensive simulation study is presented using samples of size n ($n = 50, 150, 300$ and $500|q = 95\%, 99\%$ and 99.5%) from the new IBXBXII model such that both negatively and positively skewed densities are obtained for assessing the estimators and their performance. The absolute bias and mean squared errors are used for assessing the comparison between the IBXBXII model and MOOP methodology. In relation to the data that are skewed negatively, the MOOP estimate for $\mathbb{V}_1$ performs noticeably better than the proposed IBXBXII model estimator. On the other hand, when applied to data with a positively skewed distribution, the MOOP estimator for indicator $\mathbb{V}_1$ is not superior than the proposed IBXBXII model estimate. The IBXBXII distribution clearly has a big tail to the right, as seen by the average square errors and the regression results. The provided information suggests that the new distribution is particularly suitable for insurance data that exhibits right skewness or has a long tail to the right. In such cases, the new distribution is considered more appropriate, as these characteristics indicate a more pronounced right side of the distribution. The results of simulation tests further support the conclusion that the new distribution is well-suited for mathematical modeling and actuarial risk analysis in general.

Use of AI tools declaration

The authors declare they have not used Artificial Intelligence (AI) tools in the creation of this article.

Acknowledgments

This work was supported and funded by the Deanship of Scientific Research at Imam Mohammad Ibn Saud Islamic University (IMSIU) (grant number IMSIU-RP23009).

Conflict of interest

The authors declare no conflict of interest.

References

1. I. W. Burr, Cumulative frequency functions, *Ann. Math. Stat.*, **13** (1942), 215–232. https://doi.org/10.1214/aoms/1177731607
2. I. W. Burr, On a general system of distributions, III. The simple range, *J. Am. Stat. Assoc.*, **63** (1968), 636–643.
3. I. W. Burr, P. J. Cislak, On a general system of distributions: I. Its curve-shaped characteristics; II. The sample median, *J. Am. Stat. Assoc.*, **63** (1968), 627–635. https://doi.org/10.1080/01621459.1968.11009281
4. I. W. Burr, Parameters for a general system of distributions to match a grid of 3 and 4, *Commun. Stat.*, **2** (1973), 1–21.
5. R. N. Rodriguez, A guide to the Burr-type XII distributions, *Biometrika*, **64** (1977), 129–134. https://doi.org/10.1093/biomet/64.1.129
6. P. R. Tadikamalla, A look at the Burr and related distributions, *Int. Stat. Rev.*, **48** (1980), 337–344. https://doi.org/10.2307/1402945
7. P. F. Paranaíba, E. M. Ortega, G. M. Cordeiro, R. R. Pescim, The beta Burr XII distribution with application to lifetime data, *Comput. Stat. Data An.*, **55** (2011), 1118–1136. https://doi.org/10.1016/j.csda.2010.09.009
8. P. F. Paranaiba, E. M. Ortega, G. M. Cordeiro, M. A. D. Pascoa, The Kumaraswamy Burr XII distribution: Theory and practice, *J. Stat. Comput. Sim.*, **83** (2013), 2117–2143. https://doi.org/10.1080/00949655.2012.683003
9. A. Y. Al-Saiari, L. A. Baharith, S. A. Mousa, Marshall-Olkin extended Burr type XII distribution, *Int. J. Stat. Probab.*, **3** (2014), 78–84. https://doi.org/10.5539/ijsp.v3n1p78
10. N. Alsadat, V. B. Nagarjuna, A. S. Hassan, M. Elgarhy, H. Ahmad, E. M. Almetwally, Marshall-Olkin Weibull-Burr XII distribution with application to physics data, *AIP Adv.*, **13** (2023). https://doi.org/10.1063/5.0172143
11. M. A. Zayed, A. S. Hassan, E. M. Almetwally, A. M. Aboalkhair, A. H. Al-Nefaie, H. M. Almongy, A compound class of unit Burr XII model: Theory, estimation, fuzzy, and application, *Sci. Program.*, **2023** (2023). https://doi.org/10.1155/2023/4509889
12. A. Fayomi, A. S. Hassan, H. Baaqeel, E. M. Almetwally, Bayesian inference and data analysis of the unit-power Burr X distribution, *Axioms*, **12** (2023), 297. https://doi.org/10.3390/axioms12030297
13. A. S. Hassan, E. M. Almetwally, S. C. Gamoura, A. S. Metwally, Inverse exponentiated Lomax power series distribution: Model, estimation, and application, *J. Math.*, **2022** (2022). https://doi.org/10.1155/2022/1998653

14. A. G. Abubakari, L. Anzagra, S. Nasiru, Chen Burr-Hatke exponential distribution: Properties, regressions and biomedical applications, *Comput. J. Math. Stat. Sci.*, **2** (2023), 80–105. https://doi.org/10.21608/cjmss.2023.190993.1003

15. H. M. Yousof, A. Z. Afify, G. G. Hamedani, G. Aryal, The Burr X generator of distributions for lifetime data, *J. Stat. Theory Appl.*, **16** (2017), 288–305. https://doi.org/10.2991/jsta.2017.16.3.2

16. A. Z. Afify, G. M. Cordeiro, N. A. Ibrahim, F. Jamal, M. Elgarhy, M. A. Nasir, The Marshall-Olkin odd Burr III-G family: Theory, estimation, and engineering applications, *IEEE Access*, **9** (2020), 4376–4387. https://doi.org/10.1109/ACCESS.2020.3044156

17. R. A. Bantan, C. Chesneau, F. Jamal, I. Elbatal, M. Elgarhy, The truncated Burr X-G family of distributions: Properties and applications to actuarial and financial data, *Entropy*, **23** (2021), 1088. https://doi.org/10.3390/e23081088

18. M. Haq, M. Elgarhy, S. Hashmi, The generalized odd Burr III family of distributions: Properties, and applications, *J. Taibah Univ. Sci.*, **13** (2019), 961–971. https://doi.org/10.1080/16583655.2019.1666785

19. S. K. Ocloo, L. Brew, S. Nasiru, B. Odoi, On the extension of the Burr XII distribution: Applications and regression, *Comput. J. Math. Stat. Sci.*, **2** (2023), 1–30. https://doi.org/10.21608/cjmss.2023.181739.1000

20. M. H. O. Hassan, I. Elbatal, A. H. Al-Nefaie, M. Elgarhy, On the Kavya-Manoharan-Burr X model: Estimations under ranked set sampling and applications, *J. Risk Financ. Manag.*, **16** (2023), 19. https://doi.org/10.3390/jrfm16010019

21. T. Bjerkedal, Acquisition of resistance in Guinea pigs infected with different doses of virulent tubercle bacilli, *Am. J. Hyg.*, **72** (1960), 130–148.

22. G. M. Cordeiro, H. M. Yousof, T. G. Ramires, E. M. M. Ortega, The Burr XII system of densities: Properties, regression model and applications, *J. Stat. Comput. Sim.*, **88** (2018), 432–456. https://doi.org/10.1080/00949655.2017.1392524

23. F. Figueiredo, M. I. Gomes, L. Henriques-Rodrigues, Value-at-risk estimation and the PORT mean-of-order-p methodology, *Revstat*, **15** (2017), 187–204.

24. E. Furman, Z. Landsman, Tail variance premium with applications for elliptical portfolio of risks, *ASTIN Bull. J. IAA*, **36** (2006), 433–462. https://doi.org/10.2143/AST.36.2.2017929

25. J. Havrda, F. Charvat, Quantification method of classification processes: Concept of structural entropy, *Kybernetika*, **3** (1967), 30–35.

26. Z. Landsman, On the tail mean-variance optimal portfolio selection, *Insur. Math. Econ.*, **46** (2010), 547–553. https://doi.org/10.1016/j.insmatheco.2010.02.001

27. M. D. Nichols, W. J. Padgett, A bootstrap control chart for Weibull percentiles, *Qual. Reliab. Eng. Int.*, **22** (2006), 141–151. https://doi.org/10.1002/qre.691

28. A. Rényi, *On measures of entropy and information*, In: Proceedings of the 4th Fourth Berkeley Symposium on Mathematical Statistics and Probability, Berkeley, CA, USA, **30** (1960), 547–561.

29. D. Tasche, Expected shortfall and beyond, *J. Bank. Financ.*, **26** (2002), 1519–1533. https://doi.org/10.1016/S0378-4266(02)00272-8

30. C. Acerbi, D. Tasche, On the coherence of expected shortfall, *J. Bank. Financ.*, **26** (2002), 1487–1503. https://doi.org/10.1016/S0378-4266(02)00283-2

31. C. Tsallis, The role of constraints within generalized non-extensive statistics, *Physica*, **261** (1998), 547–561.

32. M. M. A. El-Raouf, M. A. Oud, A novel extension of generalized Rayleigh model with engineering applications, *Alex. Eng. J.*, **73** (2023), 269–283. https://doi.org/10.1016/j.aej.2023.04.063

33. R. Joshi, A new picture fuzzy information measure based on Tsallis-Havrda-Charvat concept with applications in presaging poll outcome, *Comput. Appl. Math.*, **39** (2020), 71. https://doi.org/10.1007/s40314-020-1106-z

34. J. Wirch, Raising value at risk, *N. Am. Actuar. J.*, **3** (1999), 106–115. https://doi.org/10.1080/10920277.1999.10595804

35. R. Zhou, R. Cai, G. Tong, Applications of entropy in finance: A review, *Entropy*, **15** (2013), 4909–4931. https://doi.org/10.3390/e15114909

36. M. Ormos, D. Zibriczky, Entropy-based financial asset pricing, *Plos One*, **9** (2014), e115742. https://doi.org/10.1371/journal.pone.0115742

37. R. Aloui, S. B. Jabeur, H. Rezgui, W. B. Arfi, Geopolitical risk and commodity future returns: Fresh insights from dynamic copula conditional value-at-risk approach, *Resour. Policy*, **85** (2023), 103873. https://doi.org/10.1016/j.resourpol.2023.103873

38. M. Bernardi, L. Catania, Comparison of value-at-risk models using the MCS approach, *Comput. Stat.*, **31** (2016), 579–608. https://doi.org/10.1007/s00180-016-0646-6

39. Y. Dong, Z. Dong, An innovative approach to analyze financial contagion using causality-based complex network and value at risk, *Electronics*, **12** (2023), 1846. https://doi.org/10.3390/electronics12081846

40. M. I. Gomes, M. F. Brilhante, D. Pestana, *A mean-of-order-p class of value-at-risk estimators*, In: Theory and Practice of Risk Assessment: ICRA 5, Tomar, Portugal, Springer, Cham, 2015. https://doi.org/10.1007/978-3-319-18029-8_23

41. C. Trucíos, J. W. Taylor, A comparison of methods for forecasting value at risk and expected shortfall of cryptocurrencies, *J. Forecasting*, **42** (2023), 989–1007. https://doi.org/10.1002/for.2929

42. Z. Zou, Q. Wu, Z. Xia, T. Hu, Adjusted Rényi entropic value-at-risk, *Eur. J. Oper. Res.*, **306** (2023), 255–268. https://doi.org/10.1016/j.ejor.2022.08.028